The Challenge of Photochemistry for Time-Dependent Density-Functional Theory (TD-DFT)

Mark E. Casida (樫田 マーク)
Laboratoire de Chimie Théorique (LCT)
Département de Chimie Moléculaire (DCM)
Institut de Chimie Moléculaire de Grenoble (ICMG)
Université Joseph Fourier (Grenoble I)
F-38041 Grenoble
France
e-mail: Mark.Casida@UJF-Grenoble.FR
http://sites.google.com/site/markcasida/home

Advances in Electronic Structure Theory
Paris, France
Tuesday 28 April 2015
30 min.

Rhône-Alpes Associated Node

Some Memories of Andreas

April 2005: I received a mysterious package ...

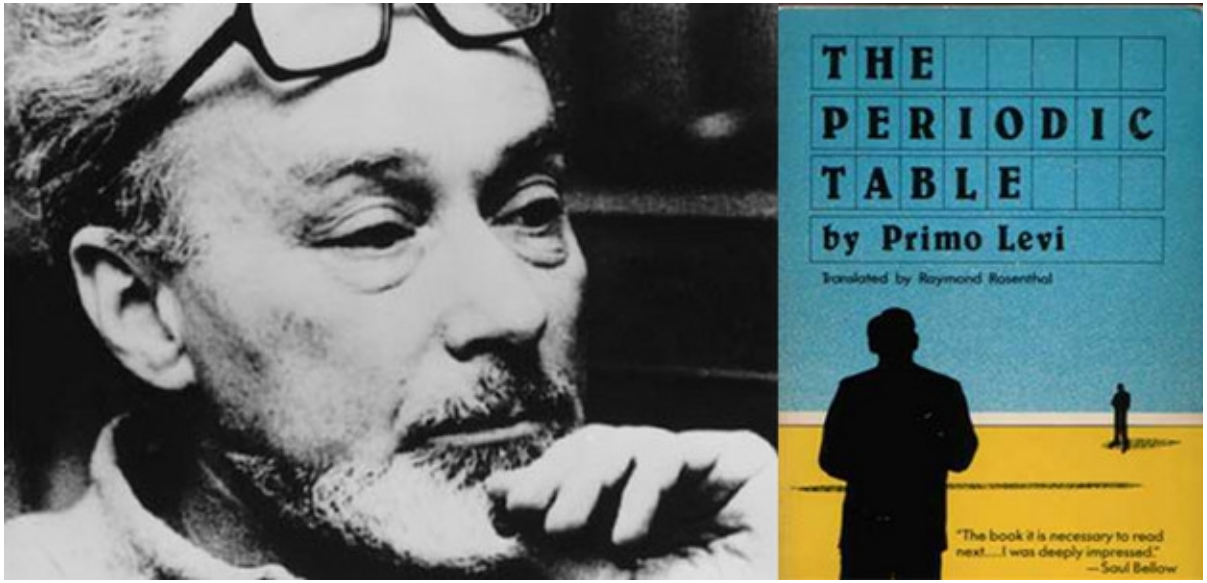

"That the chemist that I am, is now busy writing my story as a chemist, has also lived through a very different period, has been told elsewhere."

Carbon

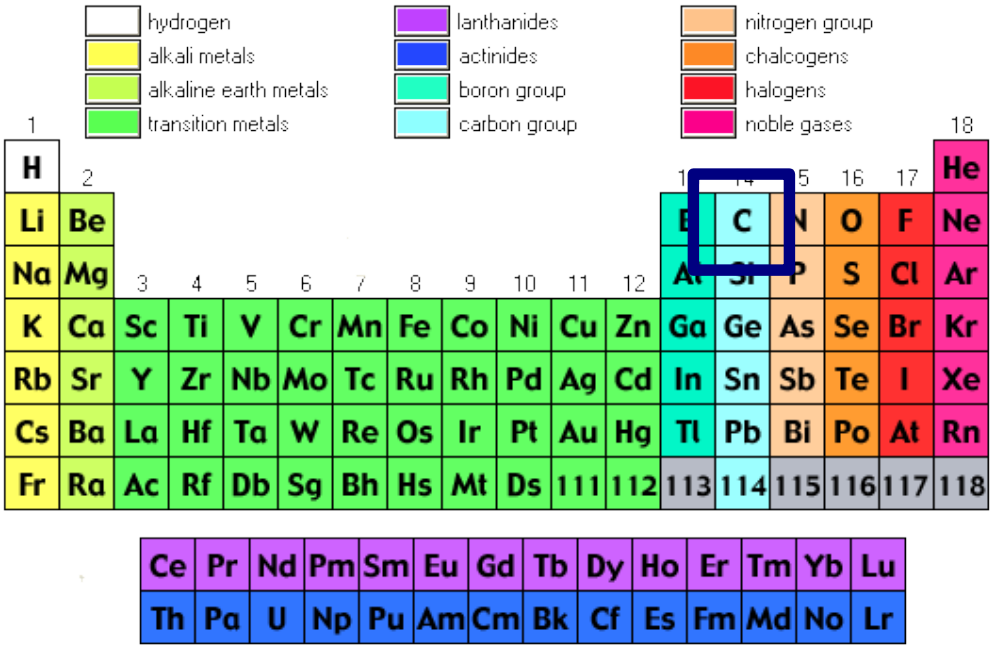

A. Savin, H. Stoll, and H. Preuss, “An application of correlation energy density functionals to atoms and molecules”, *Theor. Chim. Acta* **70**, 407 (1986)

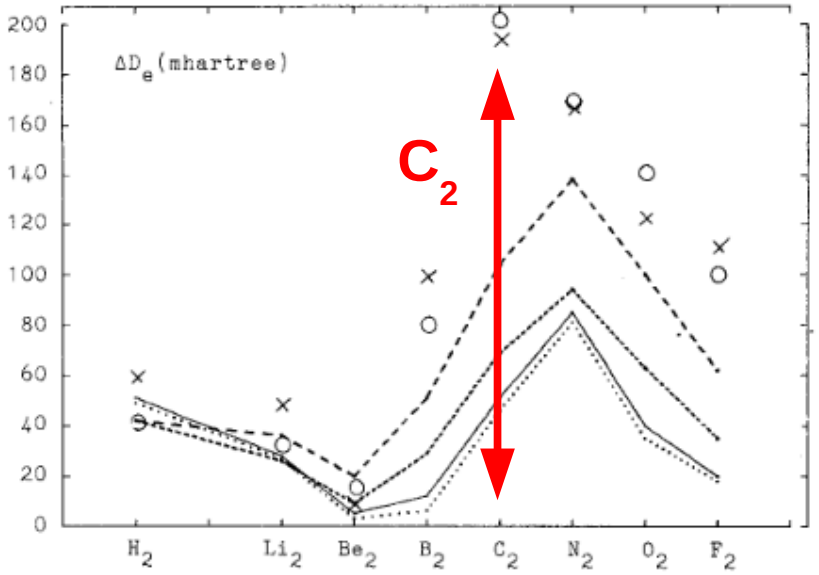

“We believe that the error can be traced back to the one-determinant restriction.”

Transition Metal Elements

We actually first met around 1989 at a meeting in Canada.

Mendeleev's original table:

Reihen	Gruppo I. — R^1O	Gruppo II. — RO	Gruppo III. — R^2O^3	Gruppo IV. RH^4 RO^2	Gruppo V. RH^3 R^2O^5	Gruppo VI. RH^2 RO^3	Gruppo VII. RH R^2O^7	Gruppo VIII. — RO^4
1	H=1							
2	Li=7	Be=9,4	B=11	C=12	N=14	O=16	F=19	
3	Na=23	Mg=24	Al=27,3	Si=28	P=31	S=32	Cl=35,5	
4	K=39	Ca=40	—=44	Ti=48	V=51	Cr=52	Mn=55	Fe=56, Co=59, Ni=59, Cu=63.
5	(Cu=63)	Zn=65	—=68	—=72	As=75	Se=78	Br=80	
6	Rb=85	Sr=87	?Yt=88	Zr=90	Nb=94	Mo=96	—=100	Ru=104, Rh=104, Pd=106, Ag=108.
7	(Ag=108)	Cd=112	In=113	Sn=118	Sb=122	Te=125	J=127	
8	Cs=133	Ba=137	?Di=138	?Ce=140	—	—	—	— — — —
9	(—)	—	—	—	—	—	—	
10	—	—	?Er=178	?La=180	Ta=182	W=184	—	Os=195, Ir=197, Pt=198, Au=199.
11	(Au=199)	Hg=200	Tl=204	Pb=207	Bi=208	—	—	
12	—	—	—	Th=231	—	U=240	—	— — — —

Oxygen

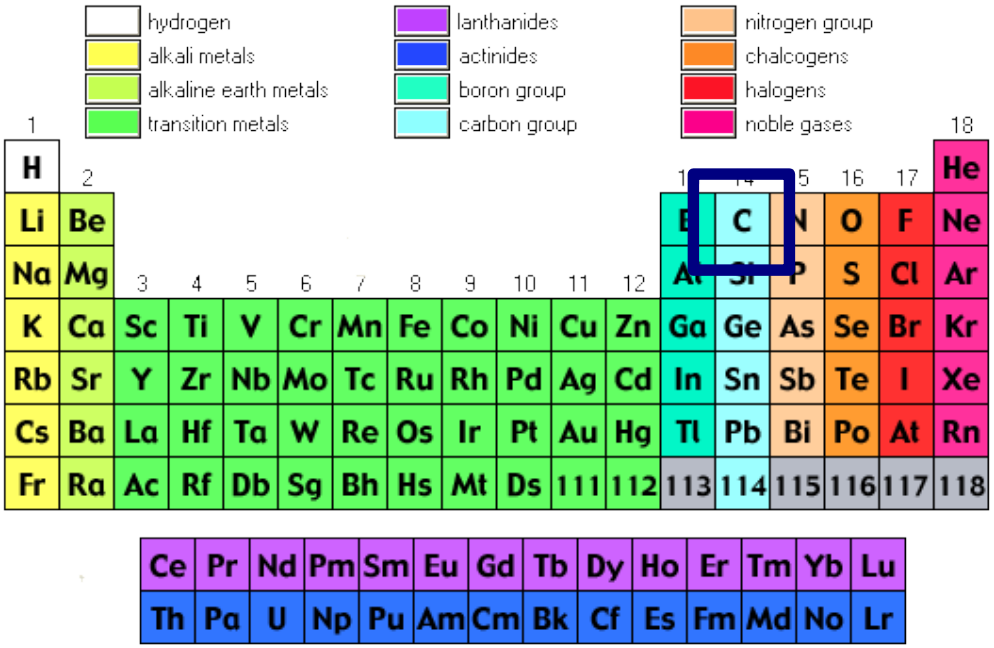

A. Savin, “Beyond the Kohn-Sham determinant”, in *Recent Advances in Density Functional Theory*, edited by D.P. Chong (World Scientific: Singapore, 1995), p. 129.

O_2 is a clear case where the single-determinant approximation must break down.

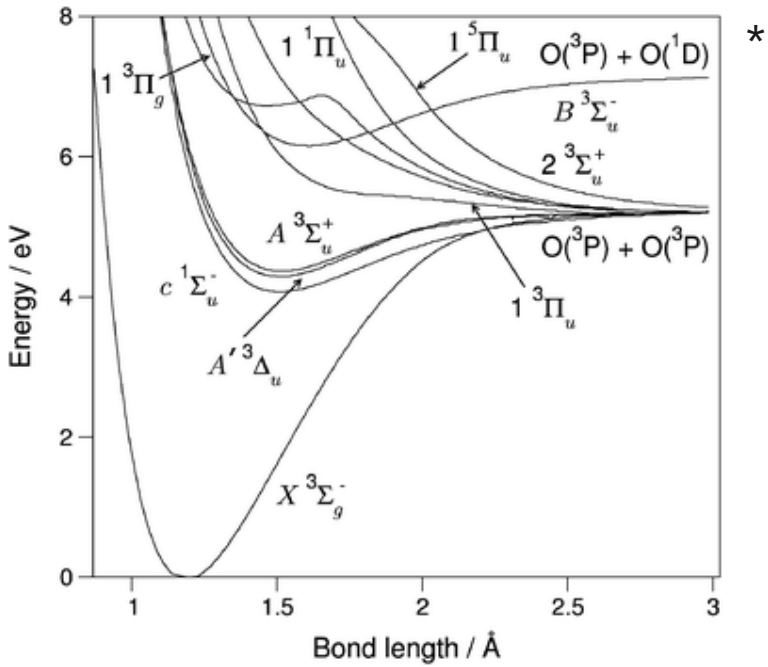

*

* graph from A.P. Clark, M. Brouard, F. Quadrini, and C. Vallance, *Phys. Chem. Chem. Phys.* **8**, 5591 (2006)

Lithium

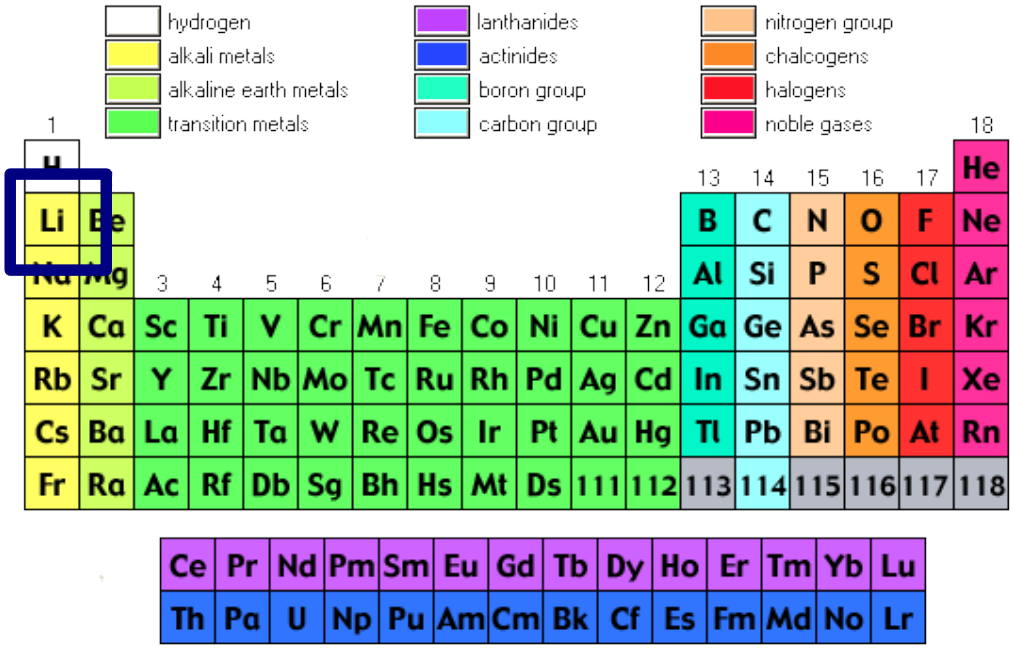

P. Fuentealba and A. Savin, "Bonding analysis of hydrogenated lithium clusters using the electron localization function", *J. Phys. Chem.* **105**, 11531 (2001).

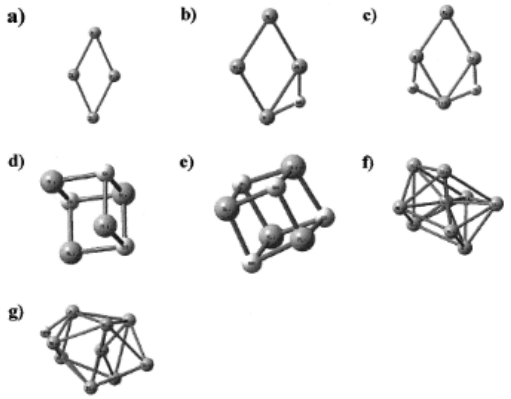

Figure 1. Geometry of the clusters, Li_nH_n with $n = 0-4$ starting from panel a until panel e. Panels f and g represent the clusters Li_9 and Li_9H, respectively.

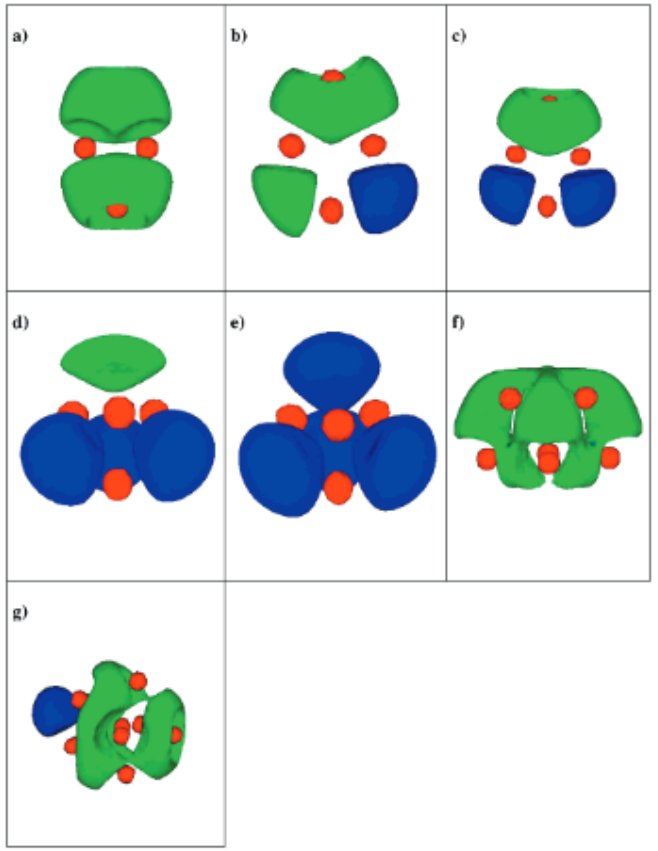

Figure 2. Isosurfaces of the electron localization function (ELF) at the value of 0.8. The panels contain the clusters in the same order as in Figure 1.

Iron

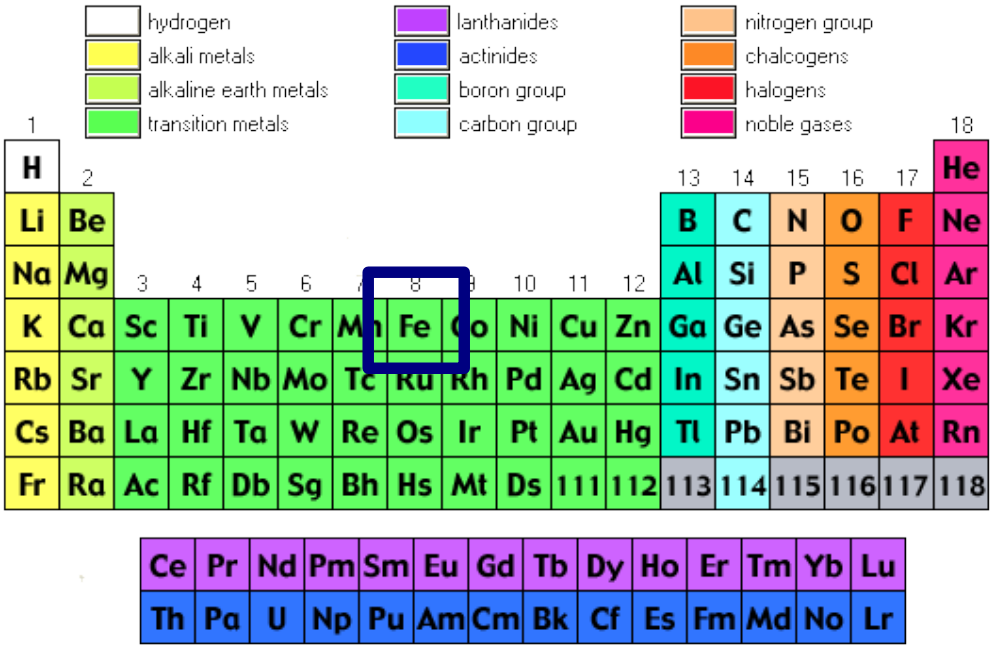

ca. 2004

Anthony Fouqueau explored applying RSHs to spin-crossover in Fe(II) complexes

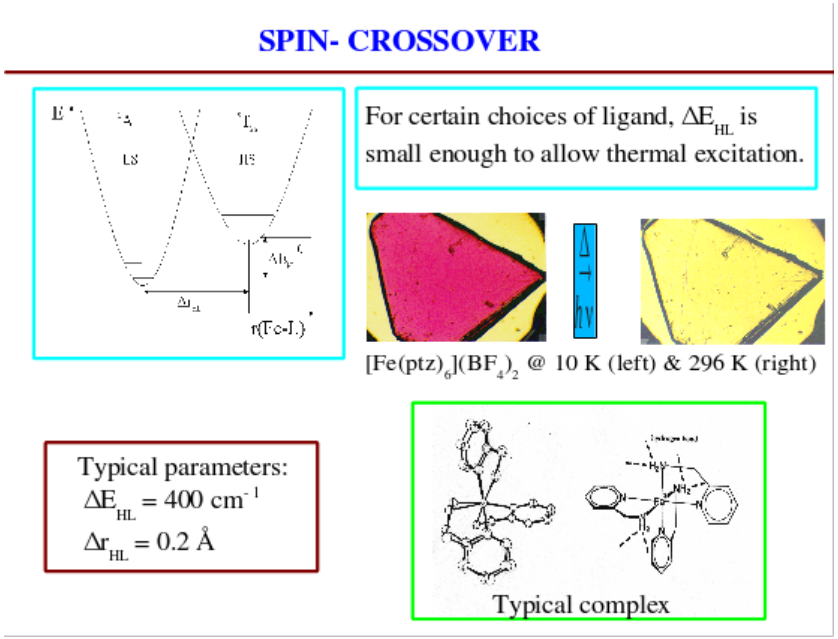

Happy 65th !

I. Gaming Levels

II. (TD-)DFT

III. Retinal Schiff Base

IV. Dressed-TD-DFT

V. Conclusions

PHOTOCHEMISTRY: A NECESSARY TOOL FOR ORGANIC SYNTHESIS

[P.E. Eaton and T.W. Cole, Jr., J. Am. Chem. Soc. 86, 962 (1964)]

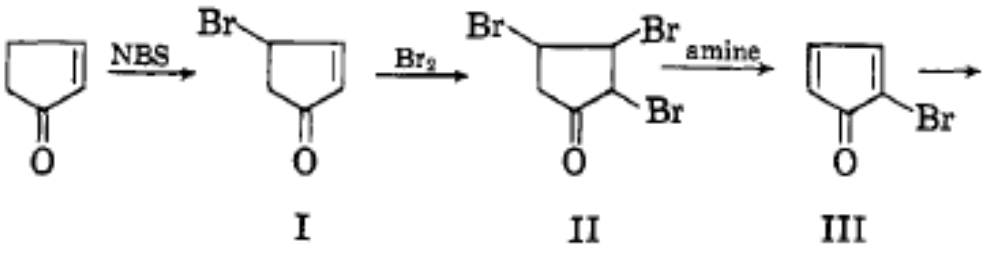

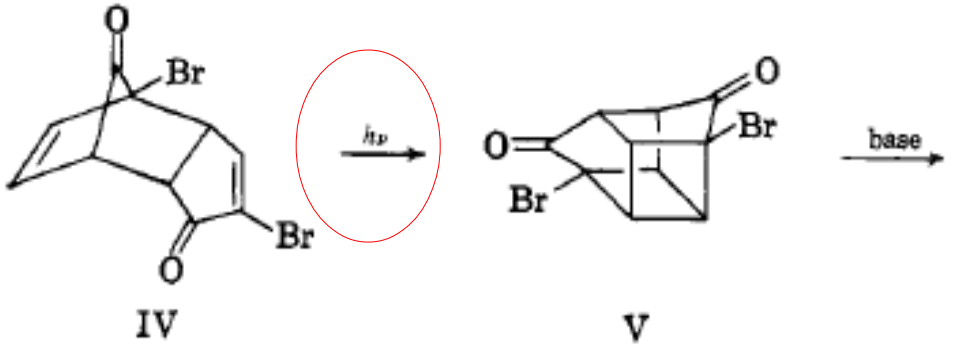

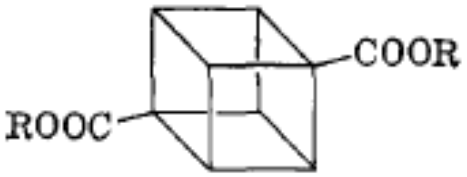

VI, R = H
VII, R = CH_3

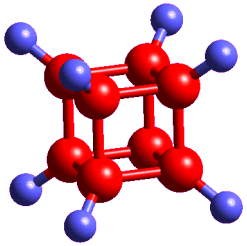

cubane

pharmaceuticals

polymers

explosives

SOME GOOD PHOTOCHEMISTRY BOOKS

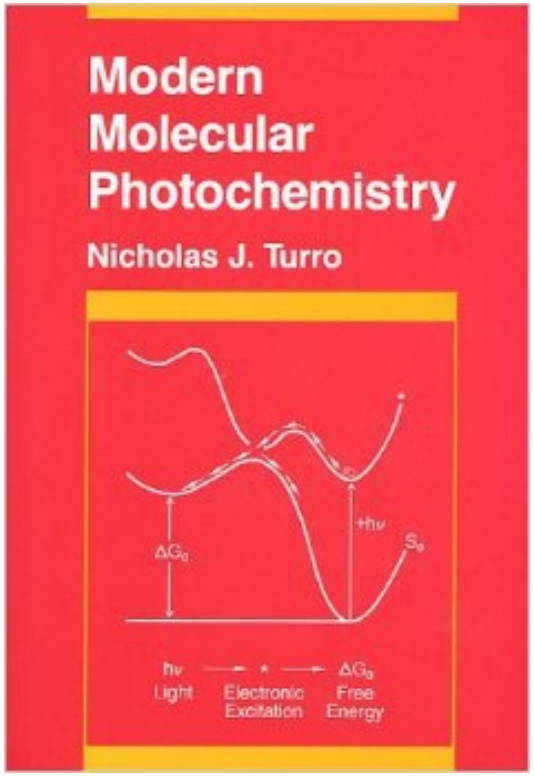

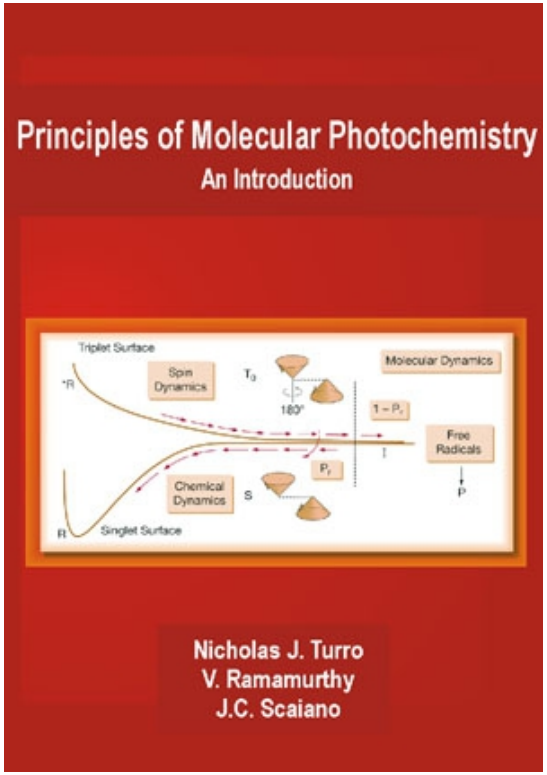

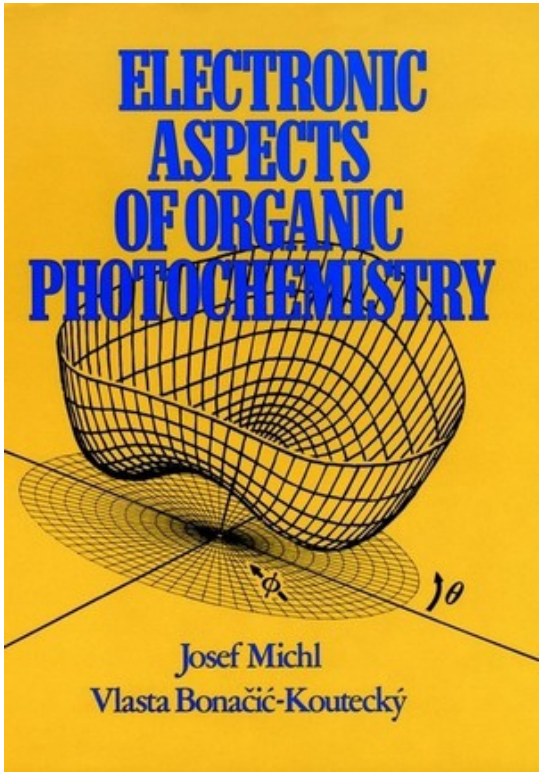

MODERN PICTURE BASED UPON POTENTIAL ENERGY SURFACES

1) **Minimum Energy Pathways (MEPs)**
2) **Dynamics**

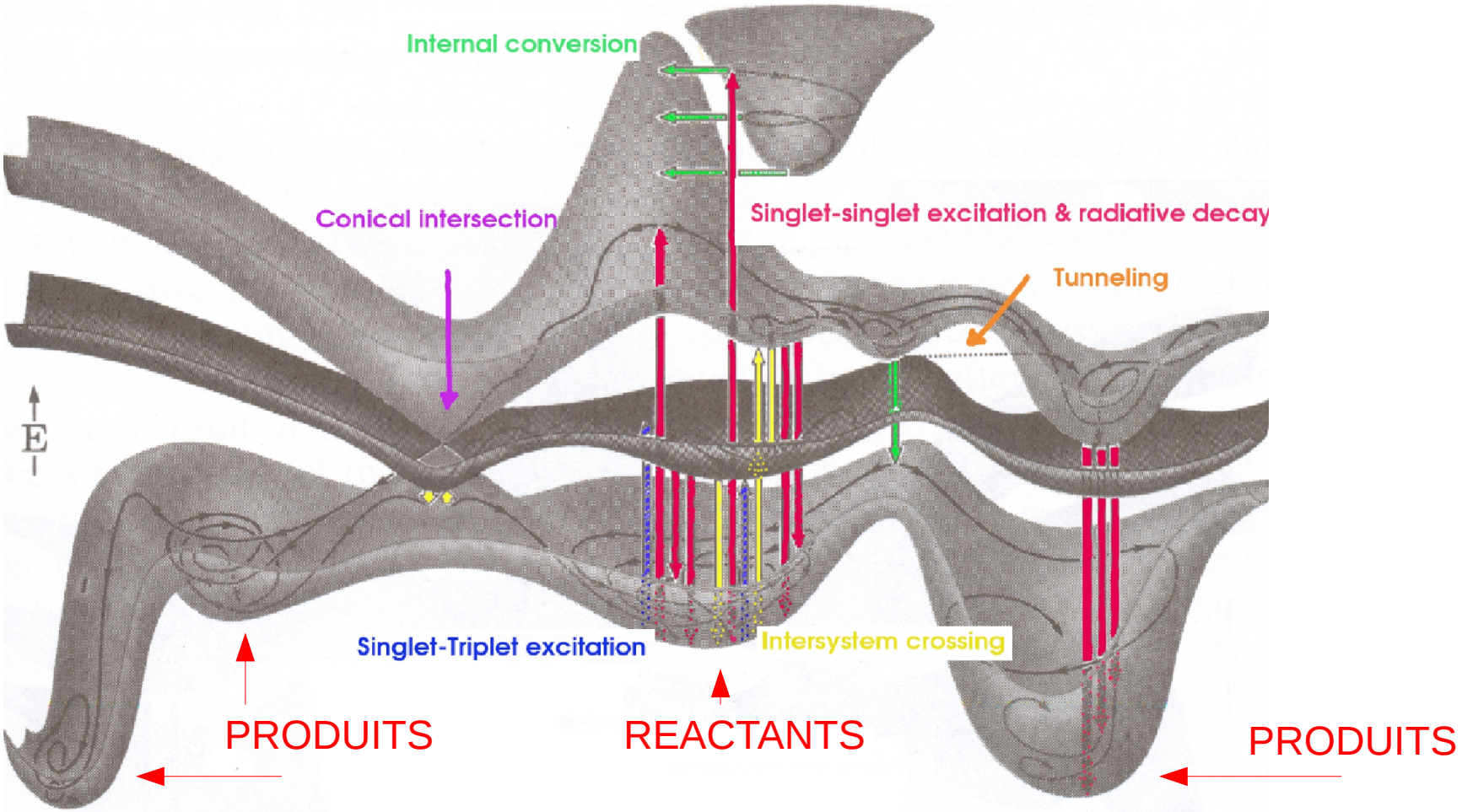

Image source: J. Michl and V. Bonacic-Koutecky, *Electronic Aspects of Organic Photochemistry* (Wiley: New York, 1990), p. 71. Embellishments: E. Tapvicza.

THE DISTINCTION BETWEEN CHEMISTRY AND PHYSICS IS WELL DEFINED HERE

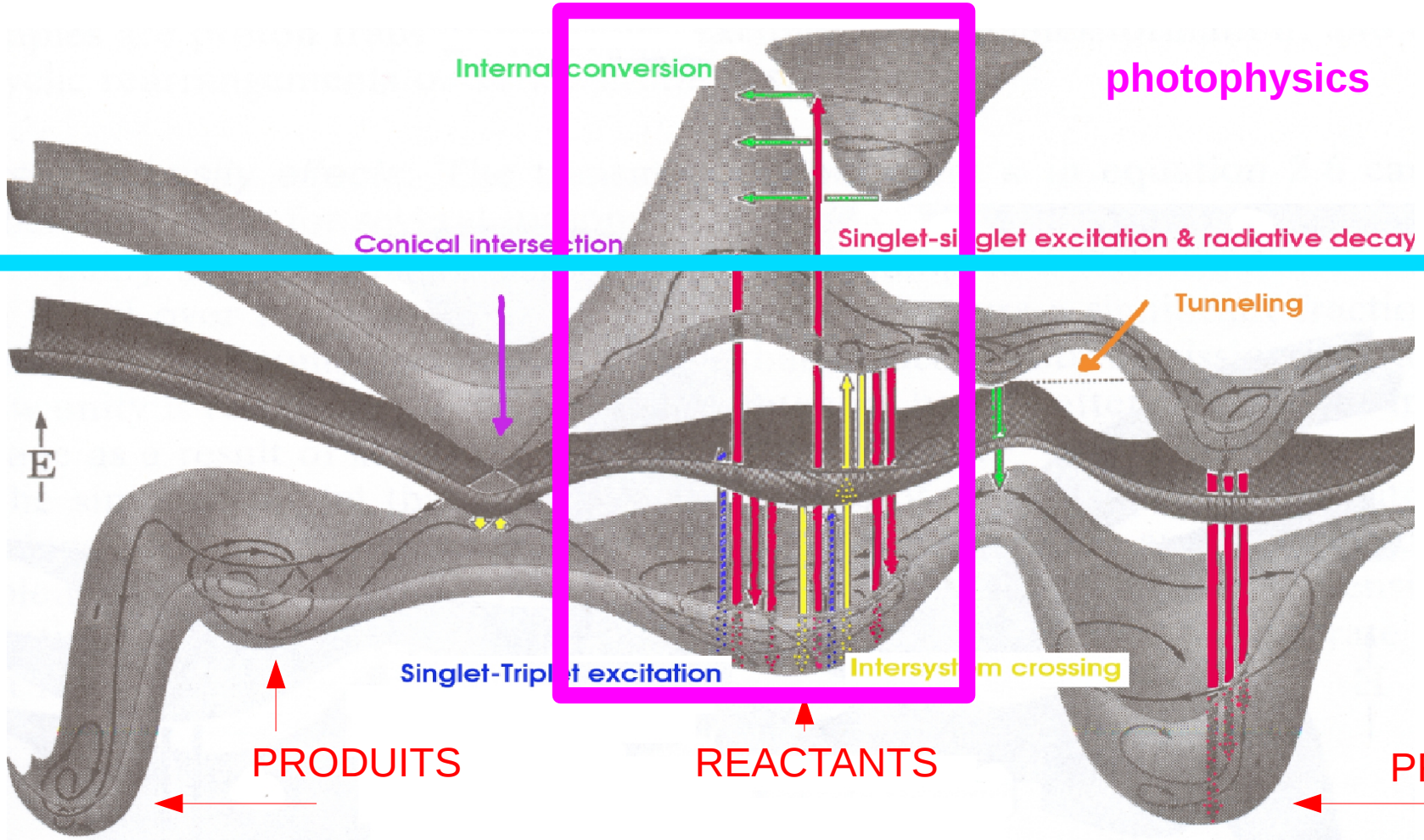

GAME RULES

- **Must get good excitation energies.**
- **Must also get good ground state energies.**
- **Excitation energies may be obtained by the response of the ground state to a time-dependent electric field.**

$$E_I = E_0 + \omega_I$$

LEVEL 1: ABSORPTION SPECTRA

Bhaarathi Natarajan

TD-LDA-TDA/wavelets

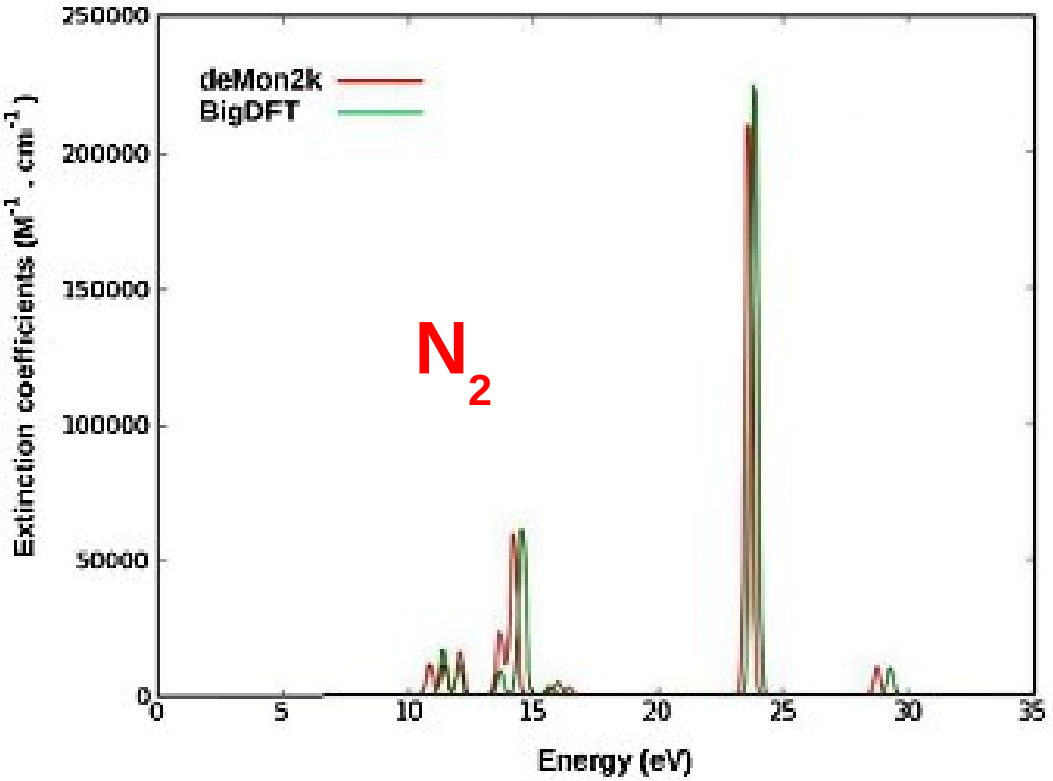

Fig. 2. Comparison of deMon2k and BigDFT N_2 spectra at higher energies.

Calculations needed to assign states.

B. Natarajan, L. Genovese, M.E. Casida, T. Deutsch, O.N. Burchak, C. Philouze, and M.Y. Balakirev, **arXiv:1108.3475v1**, *Chem. Phys.* **402**, 29 (2012); *corrigendum*, **436-437**, 63 (2014). "Wavelet-Based Linear-Response Time-Dependent Density-Functional Theory"

Potential energy curves

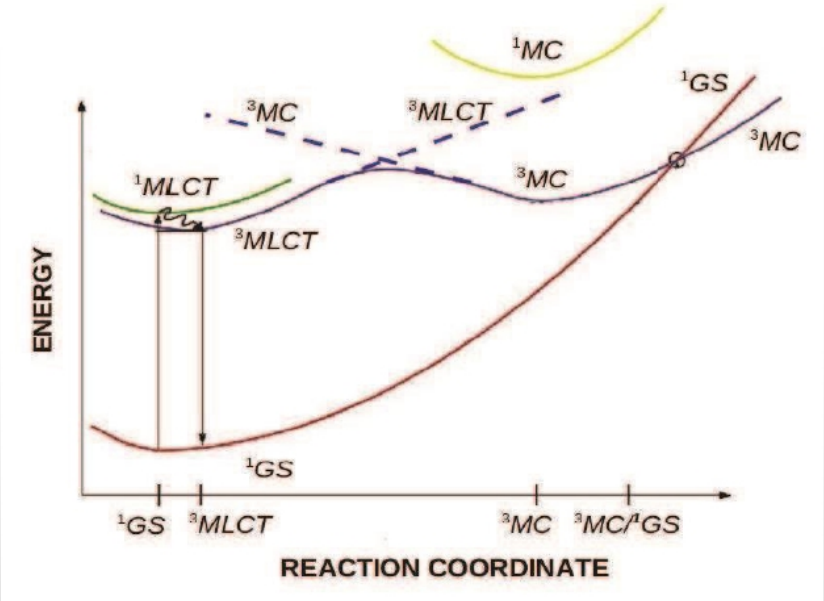

Muhavini Wawire, C., et al. Journal of Photochemistry and Photobiology A: Chemistry 276 (2013): 8-15.

11

MO luminescence indices in use

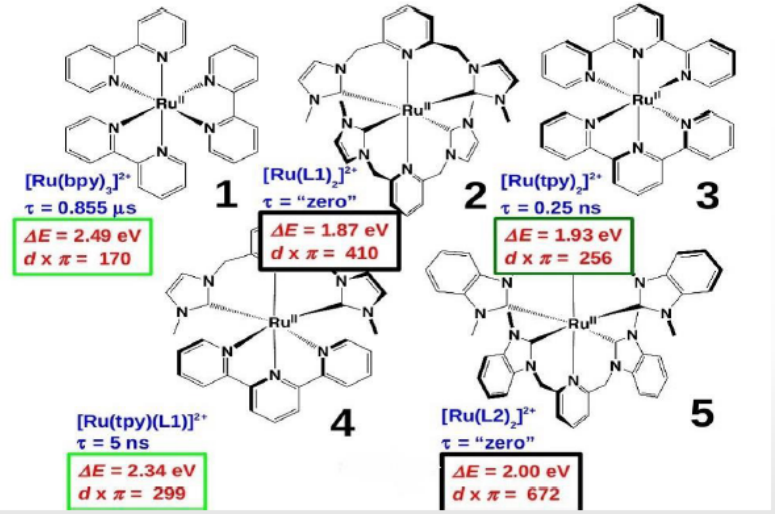

Measured luminescence lifetimes (τ) and the values of two MO-based luminescence indicators (ΔE and dxπ) for five different ruthenium complexes

Muhavini Wawire, C., et al. J. of Photochem and Photobio A: Chemistry 276 (2013): 8-15.

17

C.M. Wawire, D. Jouvenot, F. Loiseau, P. Baudin, S. Liatard, L. Njenga, G. Kamau, and M.E. Casida, *J. Photochem. and Photobiol.* **A 276**, 8 (2014). (Note that the journal has incorrectly marked 2013 instead of 2014 when they published this volume.) "Density-Functional Study of Lumininescence in Polypyridine Ruthenium Complexes"

- **Samples more of the potential energy surface.**
- **Easier to understand when the method is working or not.**

LEVEL 3: PHOTOCHEMISTRY

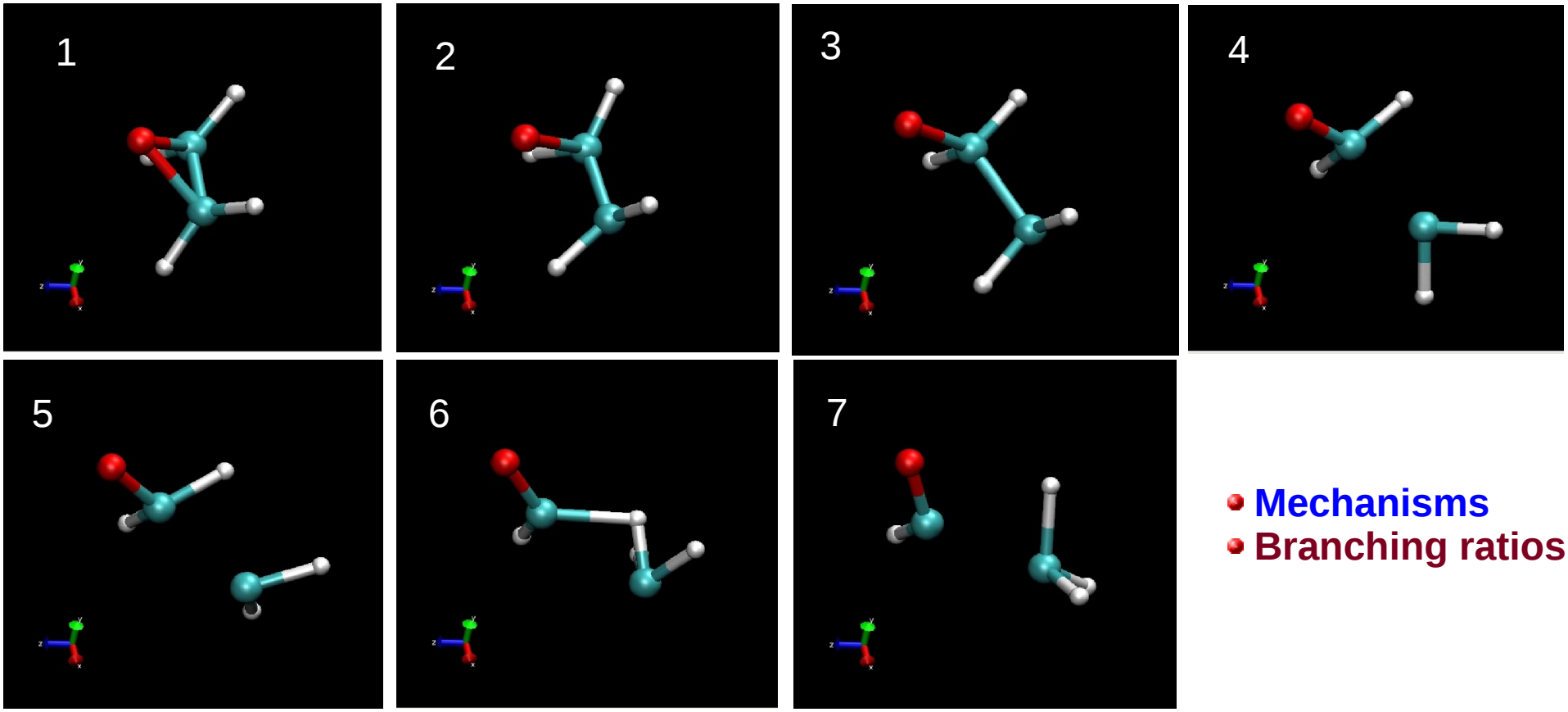

- **Mechanisms**
- **Branching ratios**

E. Tapavicza, I. Tavernelli, U. Rothlisberger, C. Filippi, and M.E. Casida, *J. Chem. Phys.* **129**, 124108 (2008). "Mixed time-dependent density-functional theory/classical surface hopping study of oxirane photochemistry"

MULTILEVEL (MODELING)

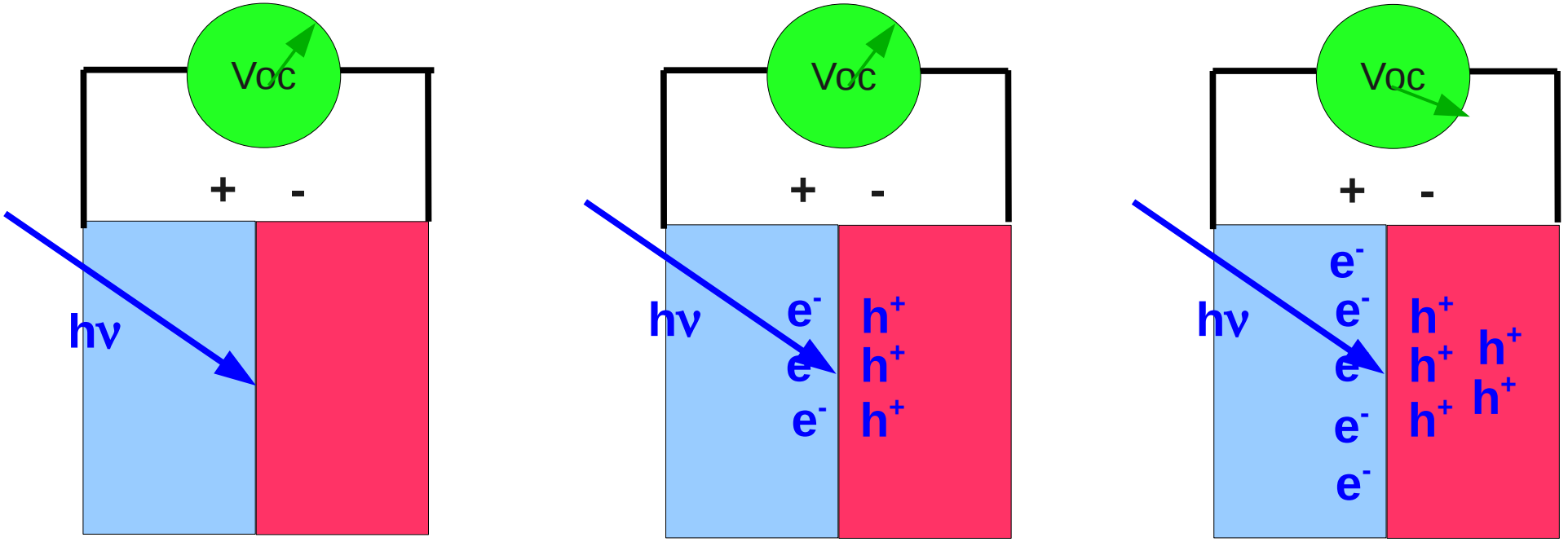

The open-circult voltage, Voc, is a function of

- The wavelength and intensity of illumination.
- The donnor HOMO/acceptor LUMO energy difference.
- The relaxation rate of the photoexcited state.
- How fast charges are conducted away from the interface.

Photobiology is another excellent candidate for multiscale modeling.

I. Gaming Levels
II. (TD-)DFT
III. Retinal Schiff Base
IV. Dressed-TD-DFT
VII. Conclusions

DFAs VERSUS DFT

Density-
Functional
Theory

- Formally exact
- Computationally useless
- What DFAs try to approximate

Density-
Functional
Approximations

- Never exact
- But computationally useful
- Try to approximate the behavior of DFT

Red bubble t-shirts http://www.redbubble.com/

Jacob's Ladder on the Abbey Church of Saint Peter and Saint Paul, Bath, England

Jacob's ladder

THEORETICAL CHEMISTRY HEAVEN

MBPT *ab initio* DFT

$\hat{K}_x^{HF}$ hybrid/OEP

$\tau(\vec{r}) = \sum_i n_i |\nabla \psi_i|^2$ mGGA*

$x(\vec{r}) = \frac{|\nabla \rho(\vec{r})|}{\rho(\vec{r})^{4/3}}$ GGA

Pure DFT

$\rho(\vec{r})$ LDA

HARTREE WORLD

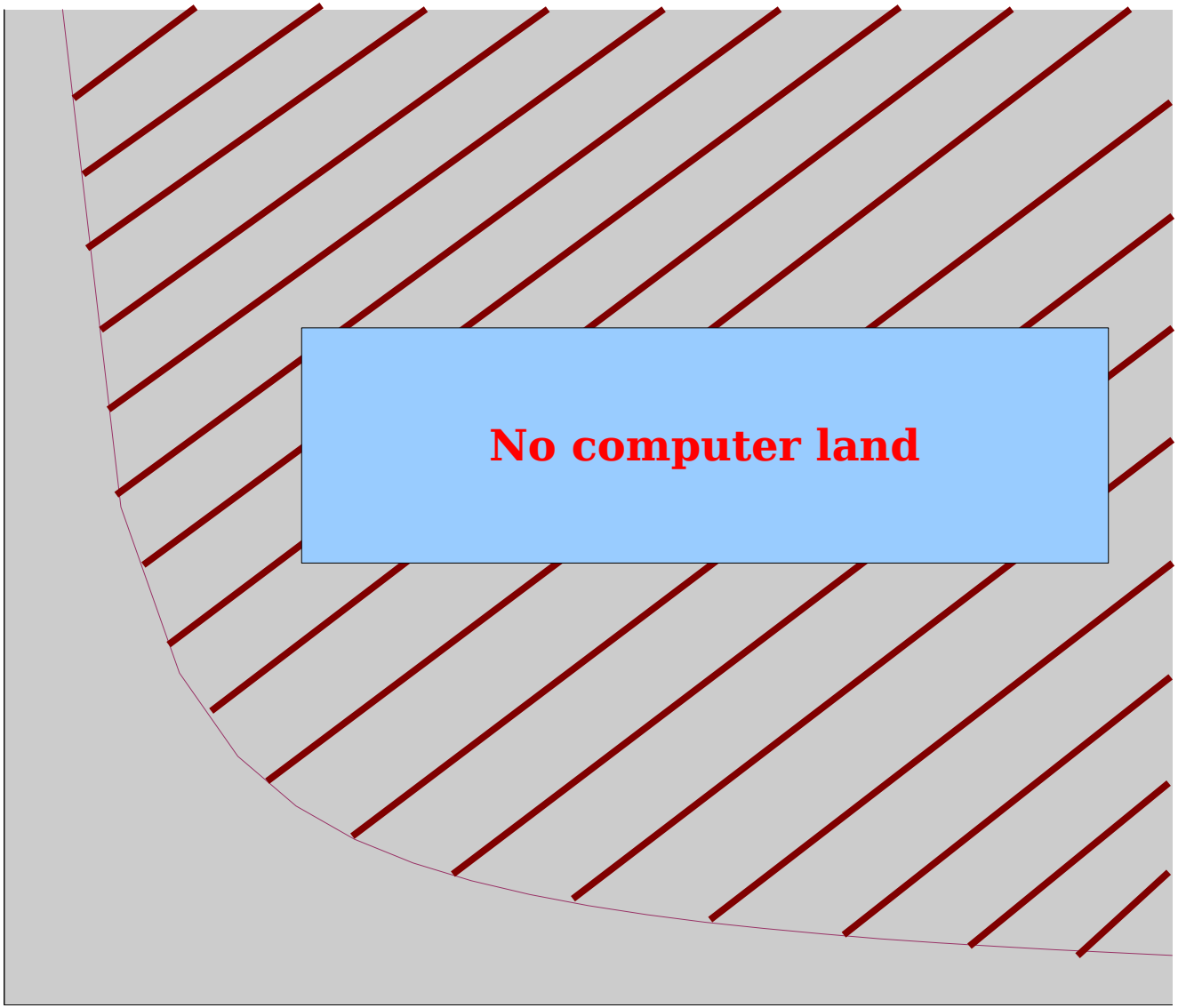

Molecular size →

* or include $\nabla^2 \rho$

Exact theory

Ground state singlet belonging to the totally symmetric irrep

$\Rightarrow \quad \rho_\alpha = \rho_\beta \quad \Rightarrow \quad v_{xc}^{\alpha} = v_{xc}^{\beta} \quad \Rightarrow$ No symmetry breaking expected!

Assumes noninteracting v-representability (NVR)

NVR: There is a fictitious Kohn-Sham system of noninteracting electrons *with integer occupation number* whose ground state gives the density of the interacting system.

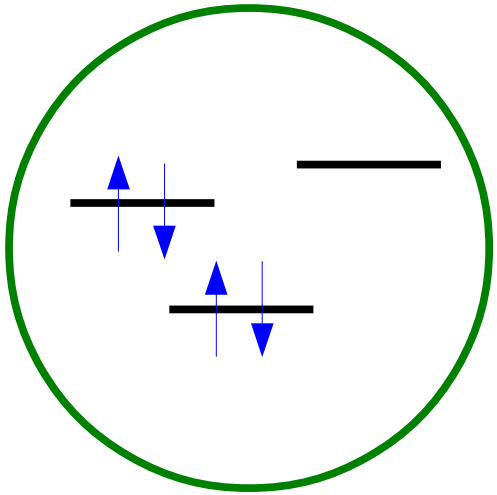

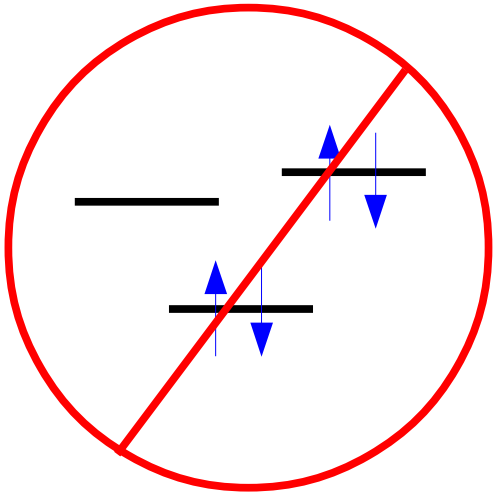

Traditional workaround is the ensemble formulation with fractional occupation numbers.

But this may lead to orbital-dependent potentials --- i.e., breakdown of the Kohn-Sham picture.

Thanks to AS and JT for the opportunity discuss with many experts !

Workshop on Range-Separated Hybrids (RSH), organized by Andreas Savin and Julien Toulouse, 9-13 May 2008, *Université Pierre et Marie Curie* (Paris VI), Jussieu Campus, Paris, France.

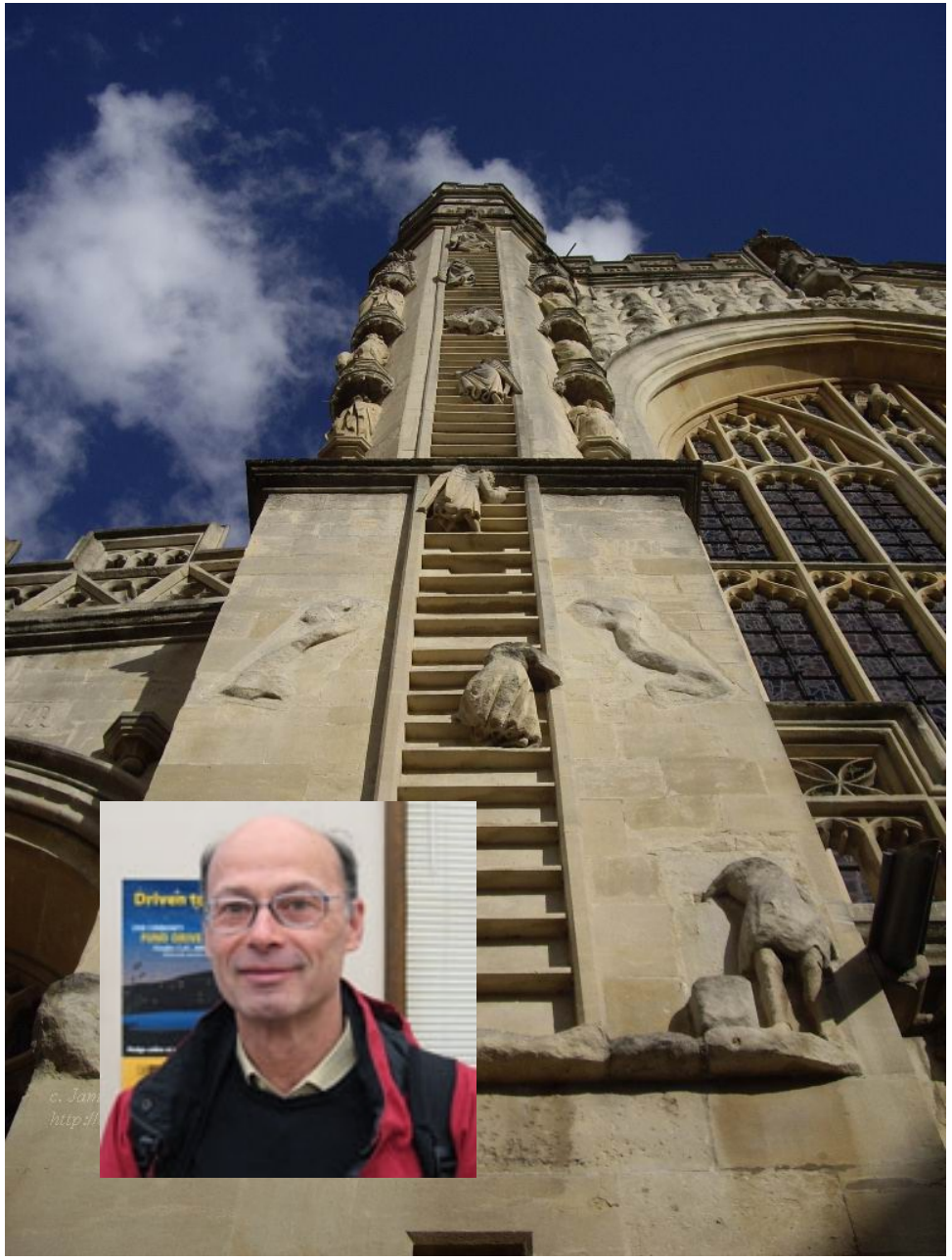

Jacob's Ladder on the Abbey Church of Saint Peter and Saint Paul, Bath, England

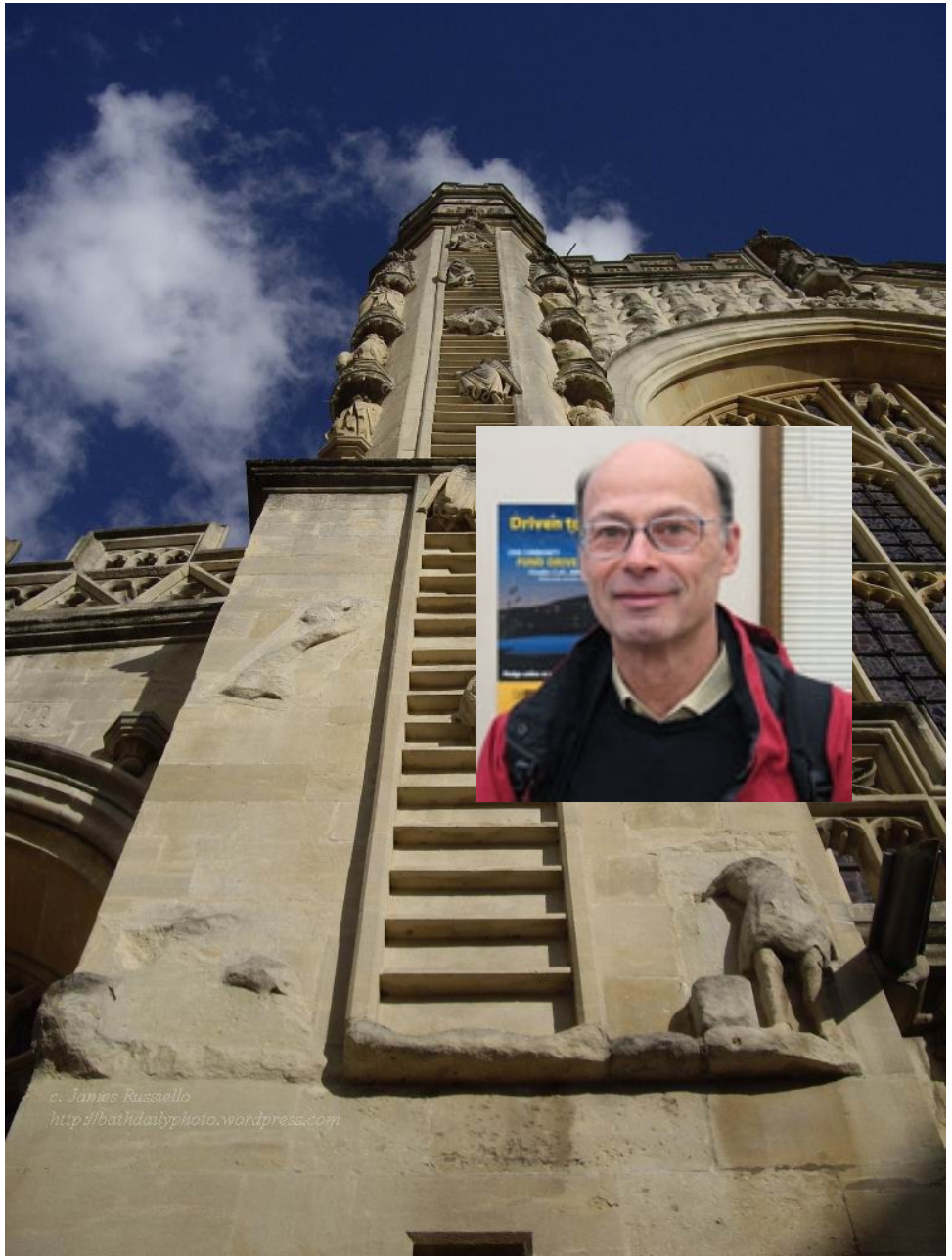

Jacob's Ladder on the Abbey Church of Saint Peter and Saint Paul, Bath, England

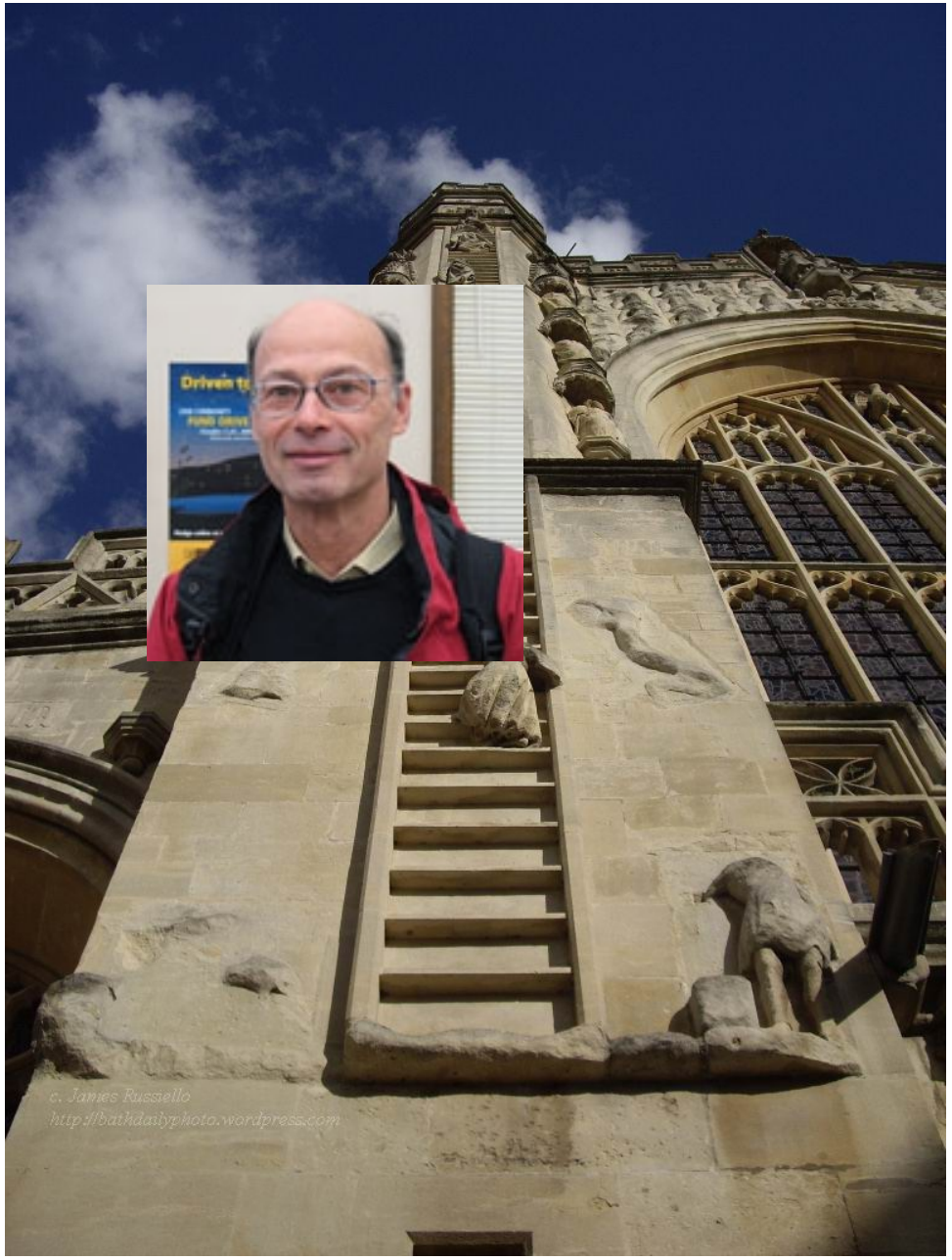

Jacob's Ladder on the Abbey Church of Saint Peter and Saint Paul, Bath, England

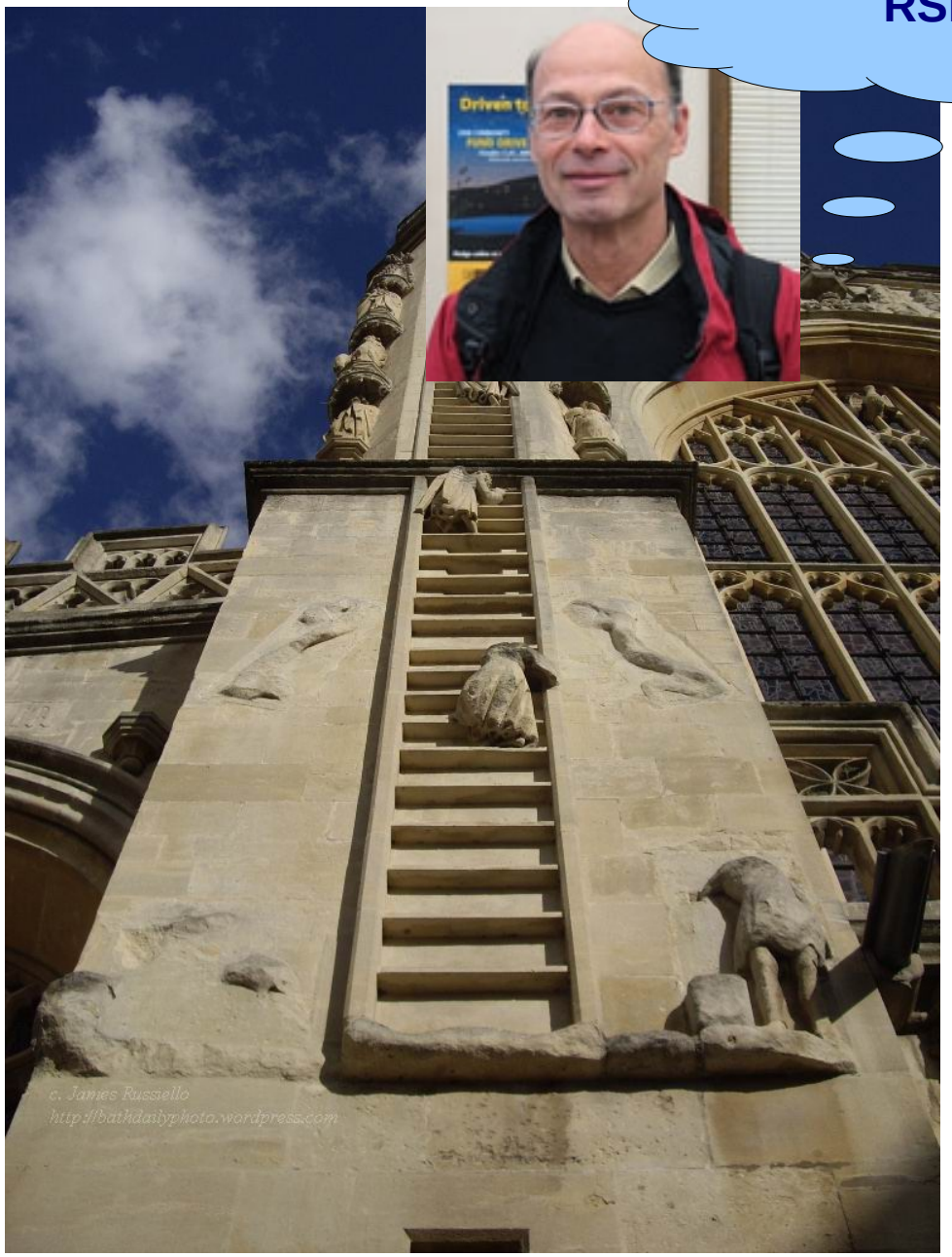

Jacob's Ladder on the Abbey Church of Saint Peter and Saint Paul, Bath, England

Range-Separated Hybrids (RSH)*

Modern GKS is
- less and less B3LYP
- more and more RSH

$$\frac{1}{r_{12}} = \underbrace{\frac{erfc(\gamma r_{12})}{r_{12}}}_{SHORT\ RANGE} + \underbrace{\frac{erf(\gamma r_{12})}{r_{12}}}_{LONG\ RANGE}$$

Molecules:
- SR <-> DFT
- LR <-> WF (e.g. HF)

Solids:
- SR <-> WF
- LR <-> DFT

Idea originally due to Andreas Savin (*Université Pierre et Marie Curie*, Paris, France.)

Applications in TDDFT:
- Y. Tawada, T. Tsuneda, S. Yanagisawa, T. Yanai, and K. Hirao, *J. Chem. Phys.* **120**, 8425 (2004).
- S. Tokura, T. Tsuneda, and K. Hirao, *J. Theoretical and Computational Chem.* **5**, 925 (2006).
- O.A. Vydrov and G.E. Scuseria, *J. Chem. Phys.* **125**, 234109 (2006).
- M.J.G. Peach, E.I. Tellgrent, P. Salek, T. Helgaker, and D.J. Tozer, *J. Phys. Chem. A* **111**, 11930 (2007).
- E. Livshits and R. Baer, *Phys. Chem. Chem. Phys.* **9**, 2932 (2007).

* Because Nature is often, *but not always*, nearsighted.

In a Nutshell

TIME-DEPENDENT DENSITY-FUNCTIONAL THEORY (TD-DFT)

For a system, initially in its ground state, exposed to time-dependent perturbation :

Runge-Gross Theorem*: $v_{ext}(\boldsymbol{r}t)$ is determined by $\rho(\boldsymbol{r}t)$ up to an additive function of time

Corollary: $\rho(\boldsymbol{r}t) \rightarrow N, v_{ext}(\boldsymbol{r}t) + C(t) \rightarrow \hat{H}(t) + C(t) \rightarrow \Psi(t) e^{-i\int_{t_0}^{t} C(t')dt'}$ (1)

van Leeuwen Theorem**: There is a system of noninteracting electrons with the same $\rho(\boldsymbol{r}t)$ but a different unique external potential $v_s(\mathbf{r}t)$ determined up to an additive function of time.

Corollary: time-dependent Kohn-Sham equation.

---

* E. Runge and E.K.U. Gross, *Phys. Rev. Lett.* **52**, 997 (1984).

** R. van Leeuwen, *Phys. Rev. Lett.* **82**, 3863 (1999).

TIME-DEPENDENT KOHN-SHAM EQUATION

$$\left[-\frac{1}{2}\nabla^2+v_{ext}(\boldsymbol{r}\,t)+\int\frac{\rho(\boldsymbol{r}\,'t)}{|\boldsymbol{r}-\boldsymbol{r}\,'|}d\boldsymbol{r}\,'+v_{xc}(\boldsymbol{r}\,t)\right]\psi_i(\boldsymbol{r}\,t)=i\frac{\partial}{\partial t}\psi_i(\boldsymbol{r}\,t) \qquad (1)$$

where $\rho(\boldsymbol{r}\,t)=\sum_{i\sigma}n_{i\sigma}|\psi_{i\sigma}(\boldsymbol{r}\,t)|^2$ (2)

and*

$$v_{xc}[\rho](\boldsymbol{r}\,t)=\frac{\delta A_{xc}[\rho]}{\delta\rho(\boldsymbol{r}\,t)}+i\langle\Psi[\rho](t_1)|\frac{\delta\Psi[\rho](t_1)}{\delta\rho(\boldsymbol{r}\,t)}\rangle-i\langle\Phi[\rho](t_1)|\frac{\delta\Phi[\rho](t_1)}{\delta\rho(\boldsymbol{r}\,t)}\rangle \qquad (3)$$

Comment: More generally, if you don't start from the ground stationary state,

$$v_{xc}(\boldsymbol{r},t)=v_{xc}[\rho,\Psi_{0,}\Phi_0](\boldsymbol{r},t) \qquad (4)$$

---

* See e.g., Carsten A. Ullrich, *Time-Dependent Density-Functional Theory* (Oxford University Press: New York, 2012), p. 114.

FREQUENCY/ENERGY FORMULATION

Mark E. Casida in *Recent Advances in Density Functional Methods, Part I,*
edited by D.P. Chong (Singapore, World Scientific, 1995), p. 155.
"Time-dependent density-functional response theory for molecules"

"RPA" equation

$$\begin{bmatrix} A(\omega_I) & B(\omega_I) \\ B(\omega_I) & A(\omega_I) \end{bmatrix} \begin{pmatrix} \vec{X}_I \\ \vec{Y}_I \end{pmatrix} = \omega_I \begin{bmatrix} 1 & 0 \\ 0 & -1 \end{bmatrix} \begin{pmatrix} \vec{X}_I \\ \vec{Y}_I \end{pmatrix} \quad (1)$$

where

$$A_{ij\sigma,kl\tau}(\omega) = \delta_{\sigma,\tau}\delta_{i,k}\delta_{j,l}(\varepsilon_{i\sigma} - \varepsilon_{j\sigma}) + K_{ij\sigma,kl\tau}(\omega) \quad (2)$$

$$B_{ij\sigma,kl\tau}(\omega) = K_{ij\sigma,lk\tau}(\omega) \quad (3)$$

Coupling matrix

$$K_{ij\sigma,kl\tau} = \int\int \psi^*_{i\sigma}(\vec{r})\psi_{j\sigma}(\vec{r}) f^{\sigma,\tau}_{Hxc}(\vec{r},\vec{r}\,';\omega)\psi_{k\tau}(\vec{r}\,')\psi^*_{l\tau}(\vec{r}\,')\, d\vec{r}\, d\vec{r}\,' \quad (4)$$

*Note: Original formulation did **not** assume the adiabatic approximation!*

Assume xc-potential responds instantaneously and without memory to any temporal change of the charge density.

$$v_{xc}(\boldsymbol{r}t) = \frac{\delta A_{xc}[\rho]}{\delta \rho(\boldsymbol{r}t)} \longrightarrow v_{xc}(\boldsymbol{r}t) = \frac{\delta E_{xc}[\rho_t]}{\delta \rho_t(\boldsymbol{r})}$$

$$\rho_t(\boldsymbol{r}) = \rho(\boldsymbol{r}t)$$

This defines "conventional TDDFT."

CONSEQUENCE OF ADIABATIC APPROXIMATION

LR-TDDFT matrix is now independent of frequency.

$$\begin{bmatrix} \boldsymbol{A} & \boldsymbol{B} \\ \boldsymbol{B} & \boldsymbol{A} \end{bmatrix} \begin{pmatrix} \vec{X}_I \\ \vec{Y}_I \end{pmatrix} = \omega_I \begin{bmatrix} \mathbf{1} & \mathbf{0} \\ \mathbf{0} & -\mathbf{1} \end{bmatrix} \begin{pmatrix} \vec{X}_I \\ \vec{Y}_I \end{pmatrix}$$

N_{occ} N_{virt} excitation solutions and N_{occ} N_{virt} de-excitation solutions.

Conclude: AA-TDDFT only gives single-electron excitations
(albeit dressed to include some correlation)

Need frequency dependence to include double excitations!

$$\begin{bmatrix} \boldsymbol{A} & \boldsymbol{B}=\boldsymbol{0} \\ \boldsymbol{B}^{*}=\boldsymbol{0} & \boldsymbol{A}^{*} \end{bmatrix} \begin{pmatrix} \vec{X} \\ \vec{Y} \end{pmatrix} = \omega \begin{bmatrix} \mathbf{1} & \mathbf{0} \\ \mathbf{0} & -\mathbf{1} \end{bmatrix} \begin{pmatrix} \vec{X} \\ \vec{Y} \end{pmatrix} \qquad (1)$$

$$\boldsymbol{A}\,\vec{X} = \omega\,\vec{X} \qquad (2)$$

Same as CIS,

$$\Psi_{trial} = \Phi\, c_0 + \sum_{i,a} a^{+}\, i\Phi\, X_{ia} \qquad (3)$$

Variational minimization leads to

Brillouin's theorem

$$\begin{bmatrix} E_{HF} & \vec{0} \\ \vec{0}^{+} & \boldsymbol{A}+E_{HF} \end{bmatrix} \begin{pmatrix} c_0 \\ \vec{X} \end{pmatrix} = E \begin{pmatrix} c_0 \\ \vec{X} \end{pmatrix} \qquad (4)$$

$$\omega = E - E_{HF} \qquad (5)$$

WHERE CONVENTIONAL TD-DFT FAILS

Mark E. Casida and Miquel Huix-Rotllant,
arXiv:1108.0611v1, *Annu. Rev. Phys. Chem.* **63**, 287 (2012).
"Progress in Time-Dependent Density-Functional Theory"

A.D. Laurent and D. Jacquemin, *Int. J. Quant Chem.* **113**, 2019 (2013).
"TD-DFT benchmarks: A review"

Mark E. Casida, *J. Mol. Struct. (Theochem)* **914**, 3 (2009).
"Review: Time-Dependent Density-Functional Theory for Molecules and Molecular Solids"

Problems reduced by the use of RSHs:

- Collapse of Rydberg states (artificially low ionization threshold)
- Under-estimated "charge-transfer" (really "density-transfer") excitations
- Scale-up catastrophe

Problems requiring memory or many-body corrections:

- Lack of double (and higher excitations)
- Topologically incorrect conical intersections
- Other coupling problems between ground and excited states

RECENT BOOKS ON TD-DFT

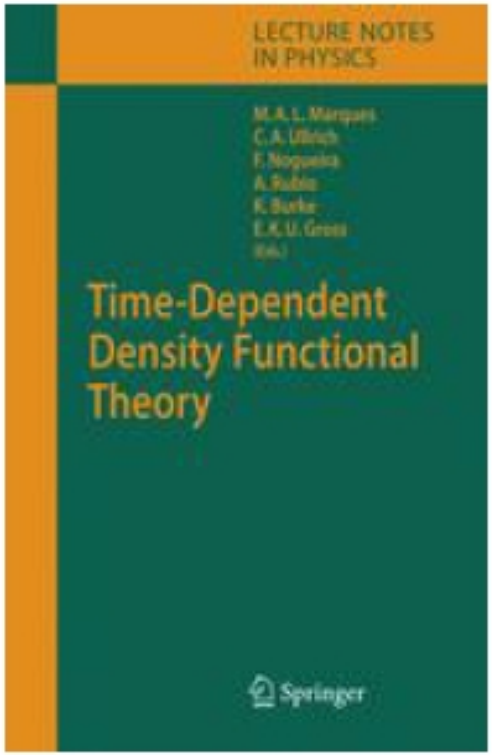

Book:
Time-Dependent Density Functional Theory, Edited by M.A.L. Marques, C.A. Ullrich, F. Nogueira, A. Rubio, K. Burke, and E.K.U. Gross, *Lecture Notes in Physics vol. 706* (Springer: Berlin, 2006).

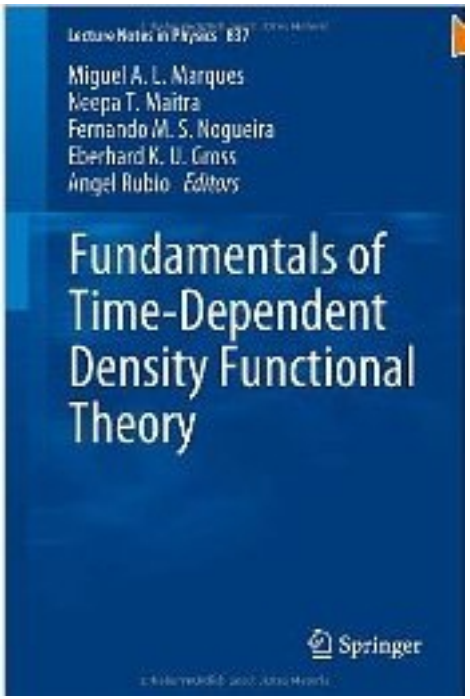

Book:
Fundamentals of Time-Dependent Density-Functional Theory, edited by M. Marques, N. Maitra, F. Noguiera, E.K.U. Gross, and A. Rubio, *Lecture Notes in Physics*, Vol. 837 (Springer: Berlin, 2011)

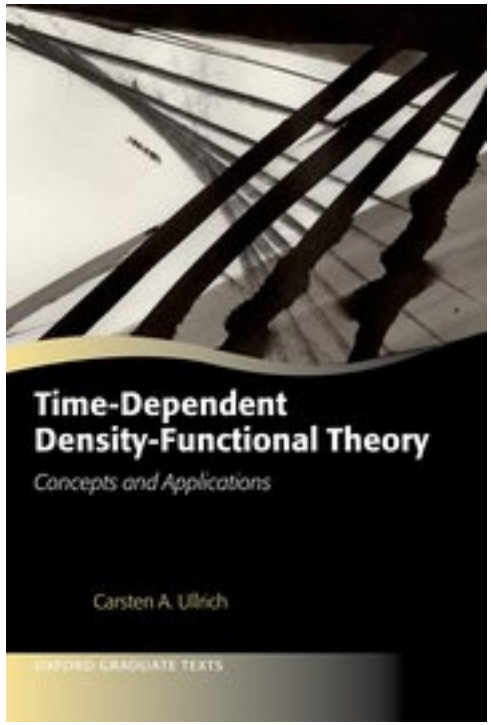

Book:
Time-Dependent Density Functional Theory, C.A. Ullrich (Oxford: 2012)

I. Gaming Levels
II. (TD-)DFT
III. Retinal Schiff Base
IV. Dressed-TD-DFT
V. Conclusions

O. Valsson, C. Filippi, and M.E. Casida, *J. Chem. Phys.* **142**, 144104 (2015)
Regarding the use and misuse of retinal protonated Schiff base photochemistry as a test case for time-dependent density-functional theory

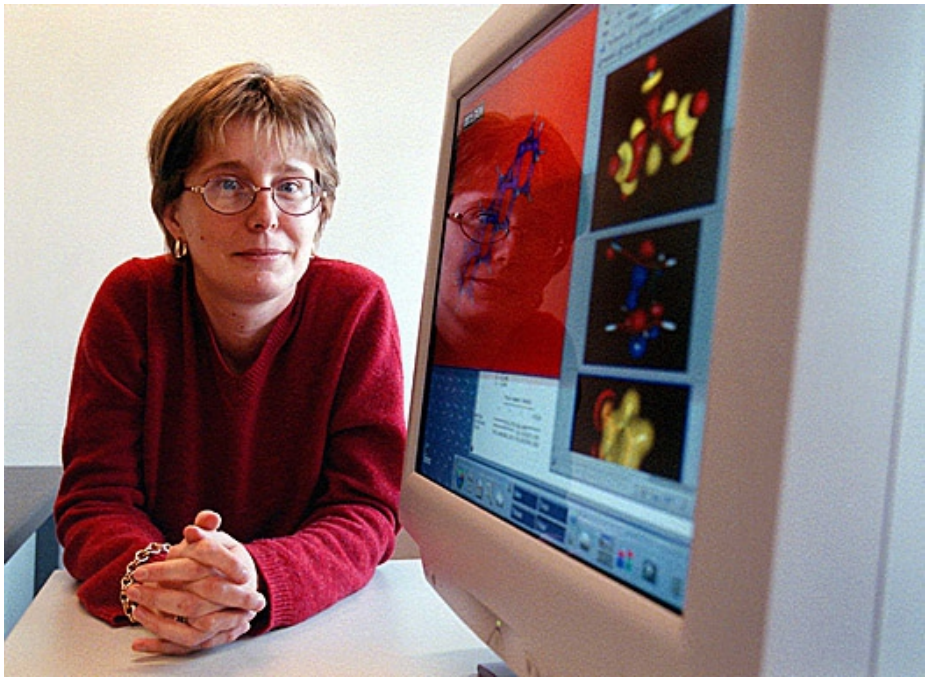

SOME BIOCHEMISTRY

Elizabeth Taylor

http://www.chm.bris.ac.uk/motm/retinal/retinalv.htm

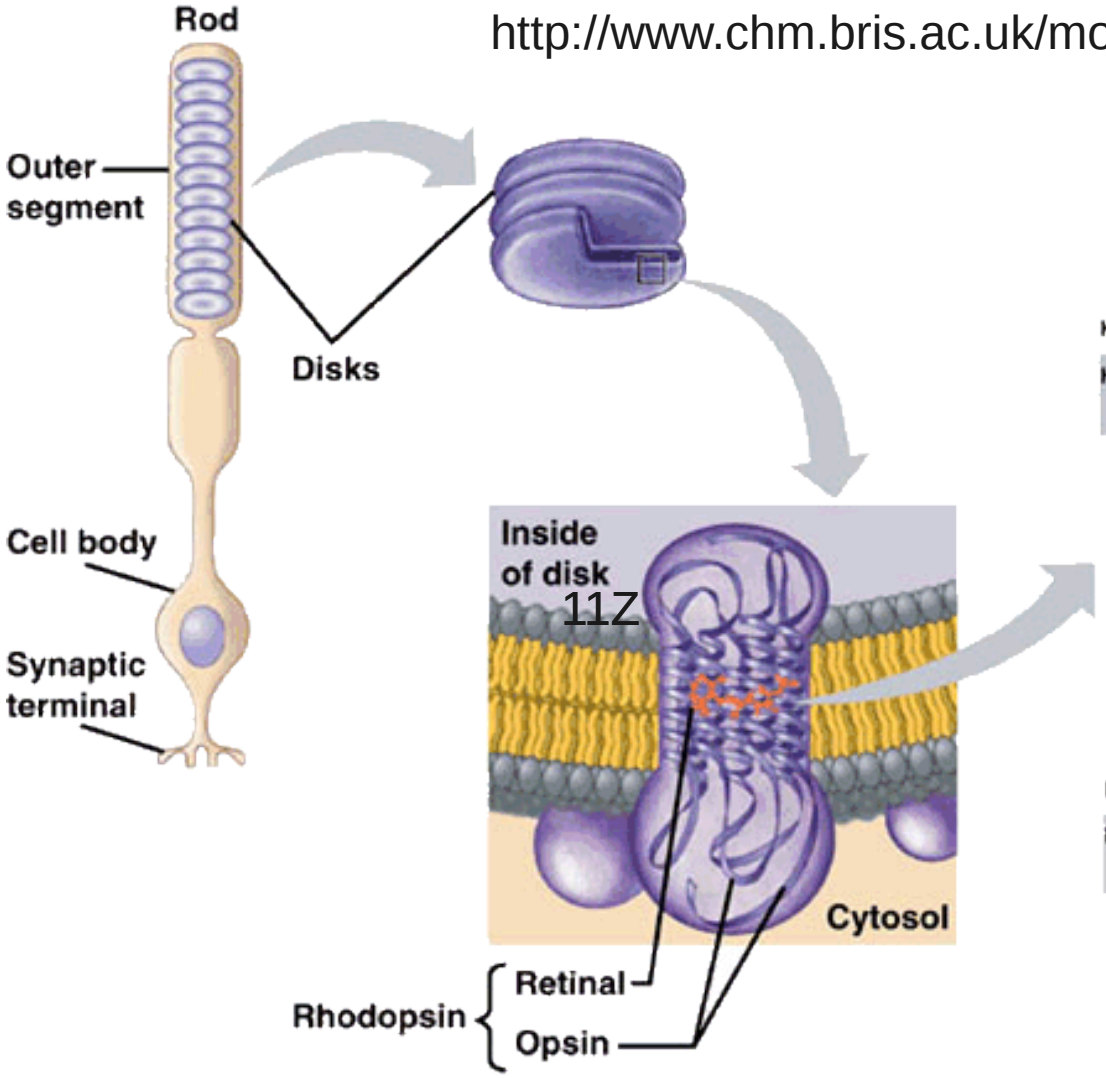

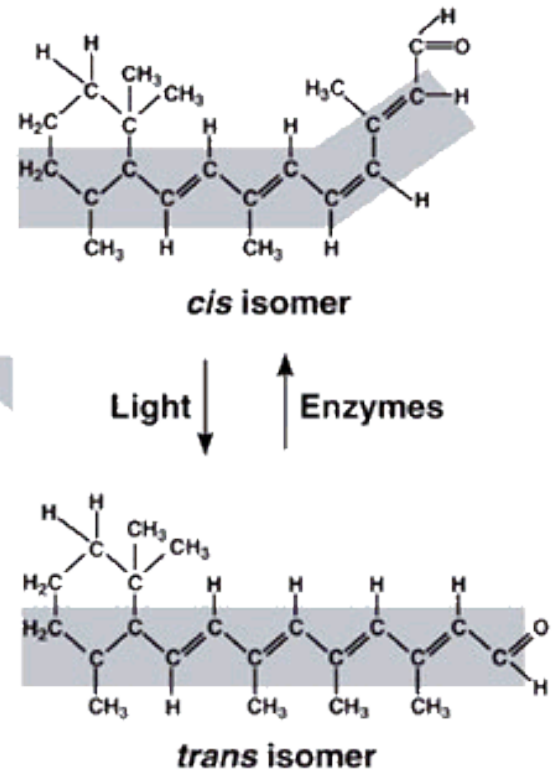

WHY APPROACH THIS WITH (TD-)DFT ?

- We want (TD-)DFT to work for large and complex systems.
- The biochemistry/physics has been particularly distrustful of TD-DFT.
- Sexy showcase application.
- Better *ab initio* calculations and experiment show that old benchmarks are “wrong”.

RETINAL PROTONATED SCHIFF BASE (PSB)

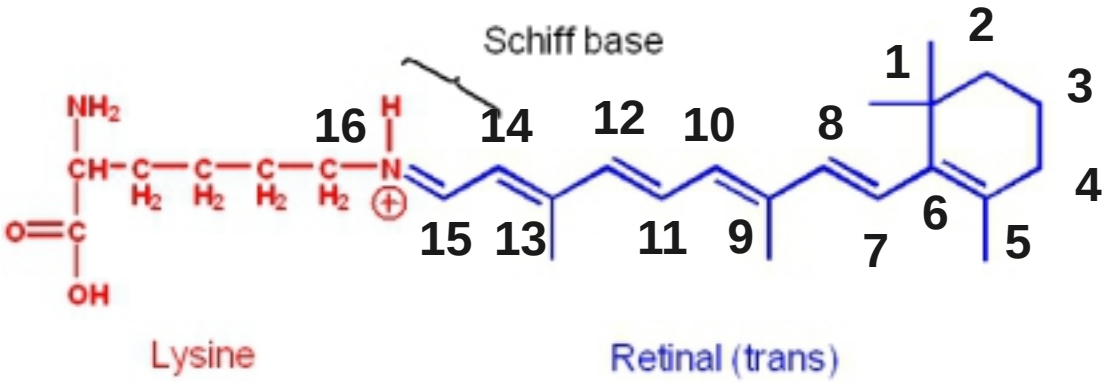

$$11Z \xrightarrow{h\nu} 11E$$

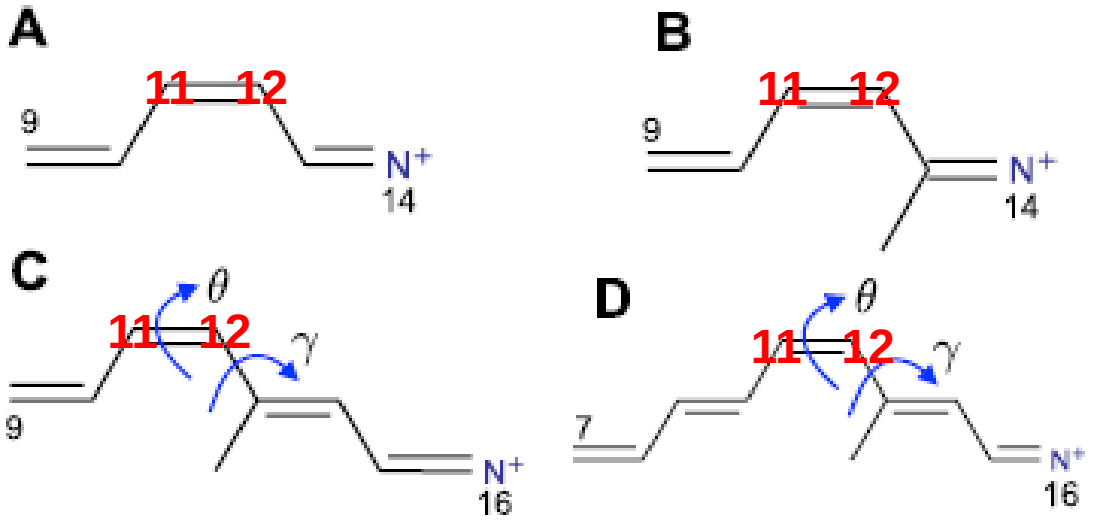

FIG. 2. Model retinal chromophores: **A** PSB3(0), **B** PSB3(1), **C** PSB4(1), and **D** PSB5(1). The naming PSBx(y) denotes the number of double bonds and methyl groups, x and y, respectively. The atom numbering for the full 11-*cis* retinal chromophore is used for all models (see Fig. S3 in the supplementary material[12]), so the *cis* bond is always between C_{11} and C_{12}. The torsional angles are defined as $\theta = \mathrm{Dih}(C_{10}–C_{11}–C_{12}–C_{13})$ and $\gamma = 180^{\circ} – \mathrm{Dih}(C_{11}–C_{12}–C_{13}–C_{14})$.

CLASSIC SINGLET MECHANISM

Fig. 1 Typical curves for the singlet photochemical isomerization of ethylene.

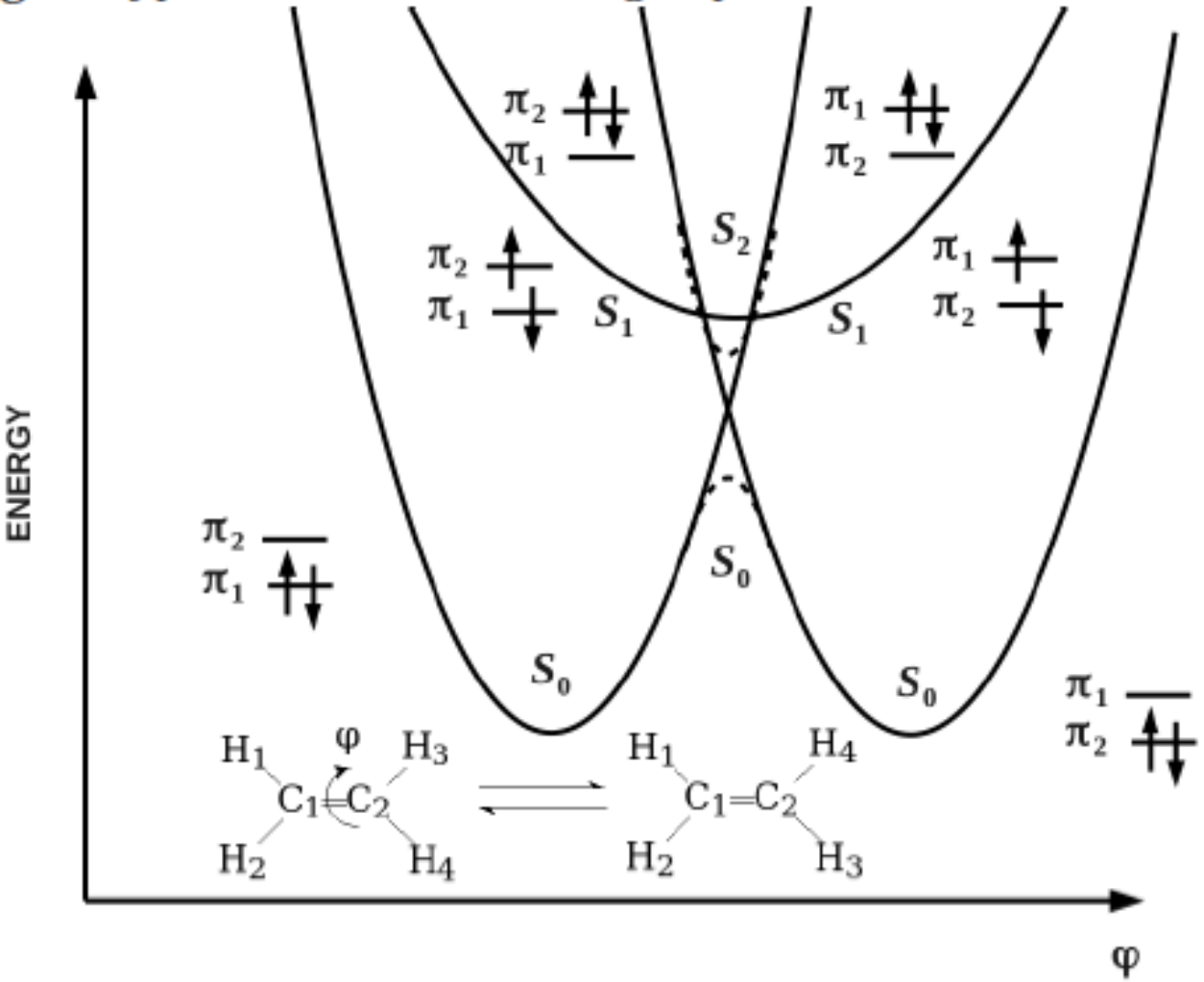

RECENT *AB INITIO* CALCULATIONS AND EXPERIMENT SAYS THAT THE PHOTOREACTION IS A BIT MORE COMPLICATED.

[GML+13] S. Gozem, F. Melaccio, R. Lindh, A.I. Krylov, A.A. Granovsky, C. Angeli, and M. Olivucci, *J. Chem. Theory Comput.* **9**, 4495 (2013). "Mapping the excited state potential energy surface of a retinal chromophore model with multireference ane equation-of-motion coupled cluster methods"

[SKS11] R. Send, V.R.I. Kaila and D. Sundholm, *J. Chem. Theory Comput.* **7**, 2473 (2011). "Benchmarking the approximate second-order coupled cluster method on biochromophores"

[VF10] O. Valsson and C. Filippi, *J. Chem. Theory Comput.* **6**, 1275 (2010). "Photoisomerization of model retinal chromophores: Insight with Quantum Monte Carlo and multiconfiguration perturbation theory"

[ZHC09] G. Zgrablić, S. Haacke, and M. Chergui, *J. Phys. B* **113**, 4384 (2009). "Heterogeneity and relaxation dynamics of the photoexcited retinal Schiff base cation in solution"

Warning: trans → cis

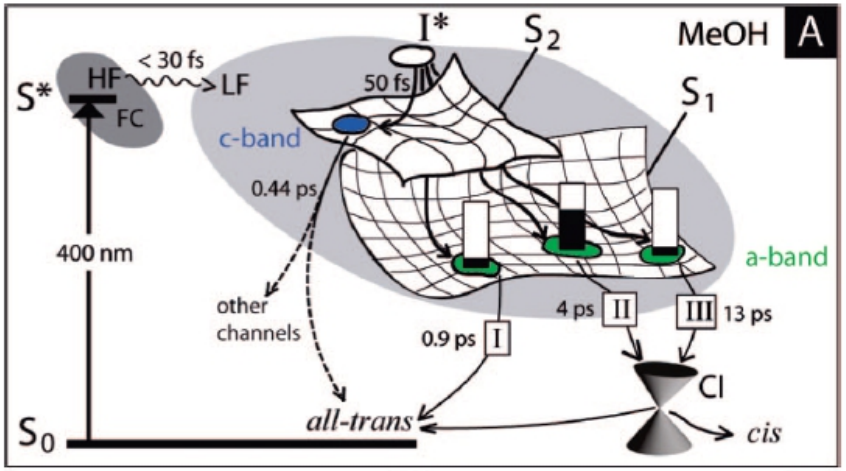

Bond Length Alternation (BLA)

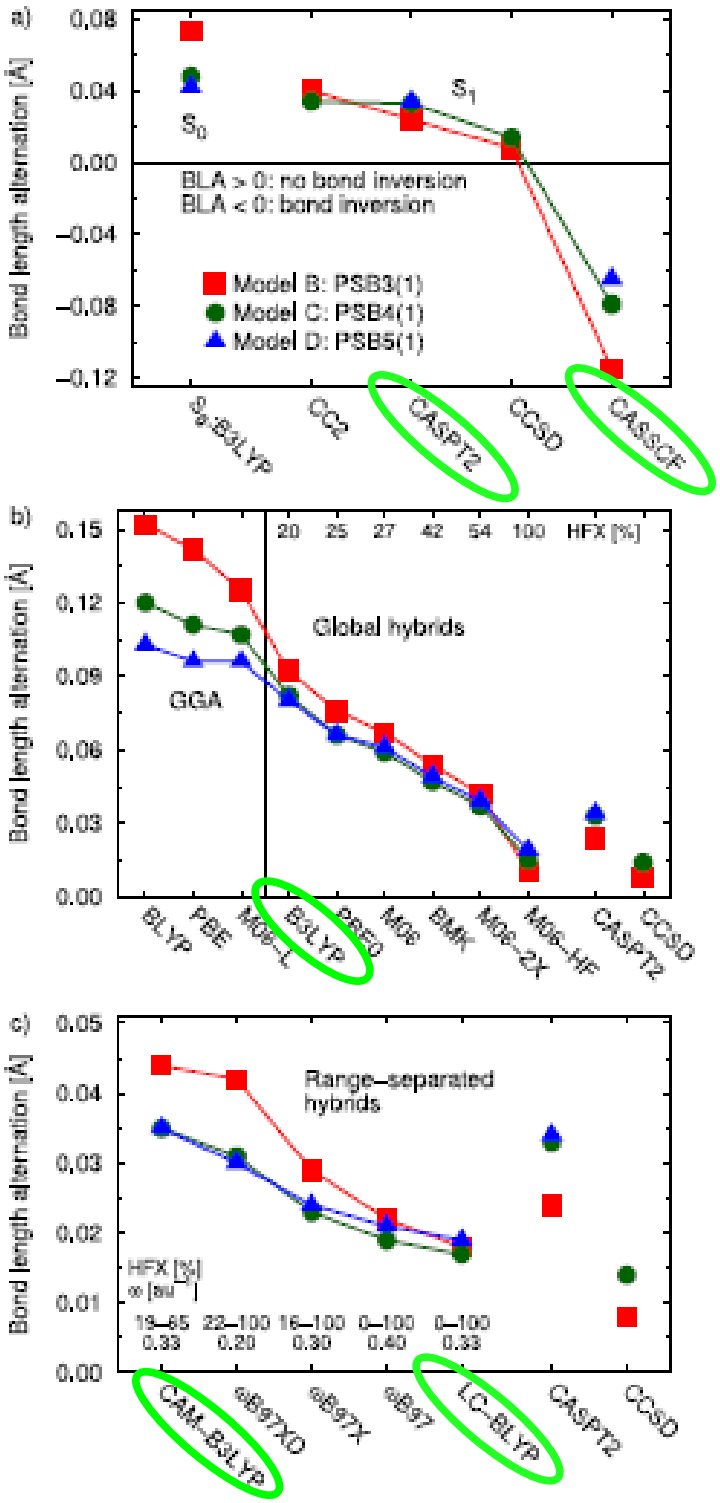

BLA = < R(C-C) > - < R(C=C) >
where C-C and C=C refer to the ground state.

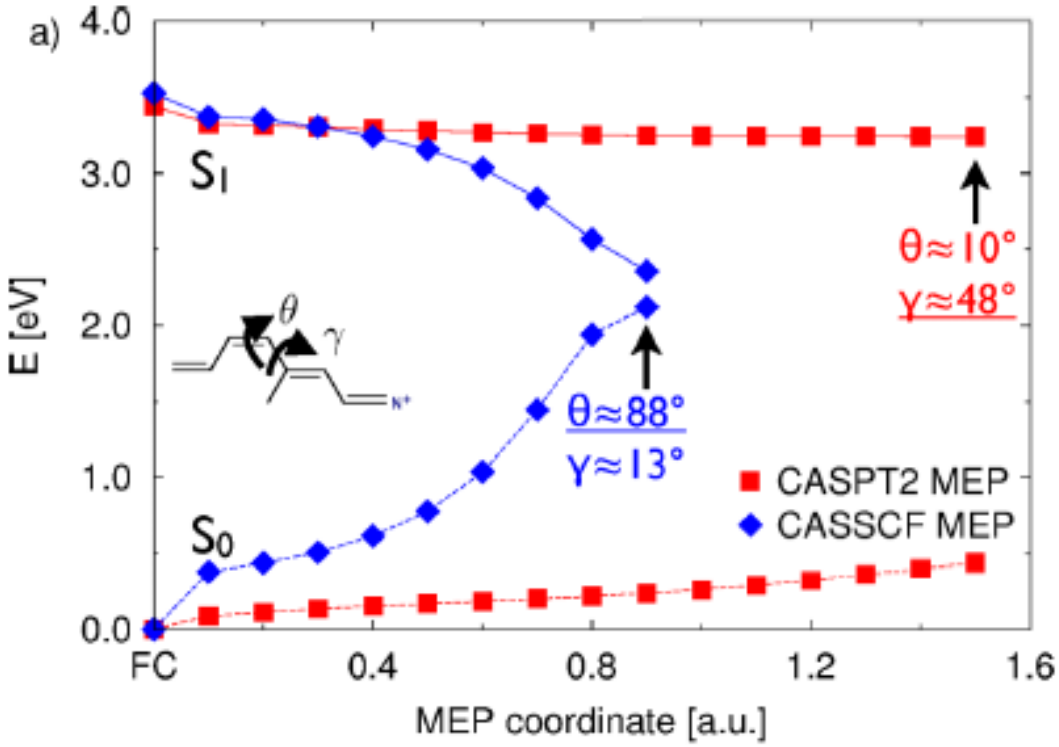

d = double bond in ground state

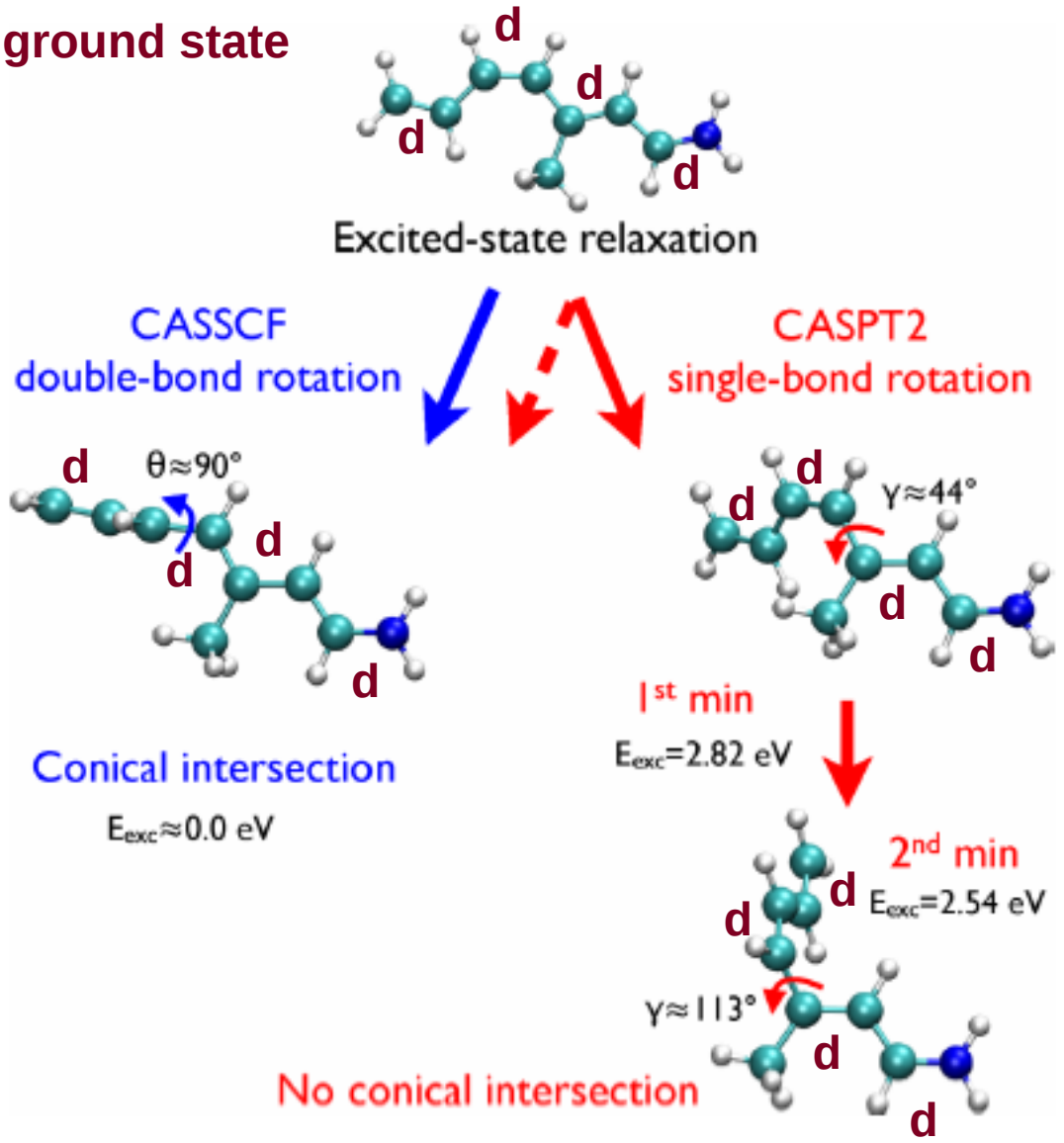

FIG. 1. The excited-state out-of-plane minima obtained with CASSCF and CASPT2. The solid arrows indicate MEPs while the dashed (red) arrow indicates the presence of a transition state on the S_1 surface.

Classical mechanism only accessed after surmounting an excited-state activation barrier.

Dynamic correlation leads to a floppy excited state with more equal bond lengths and rotations around "double bonds".

d = double bond in ground state

CASSCF

$\theta = 93^o$

$\gamma = 0^o$

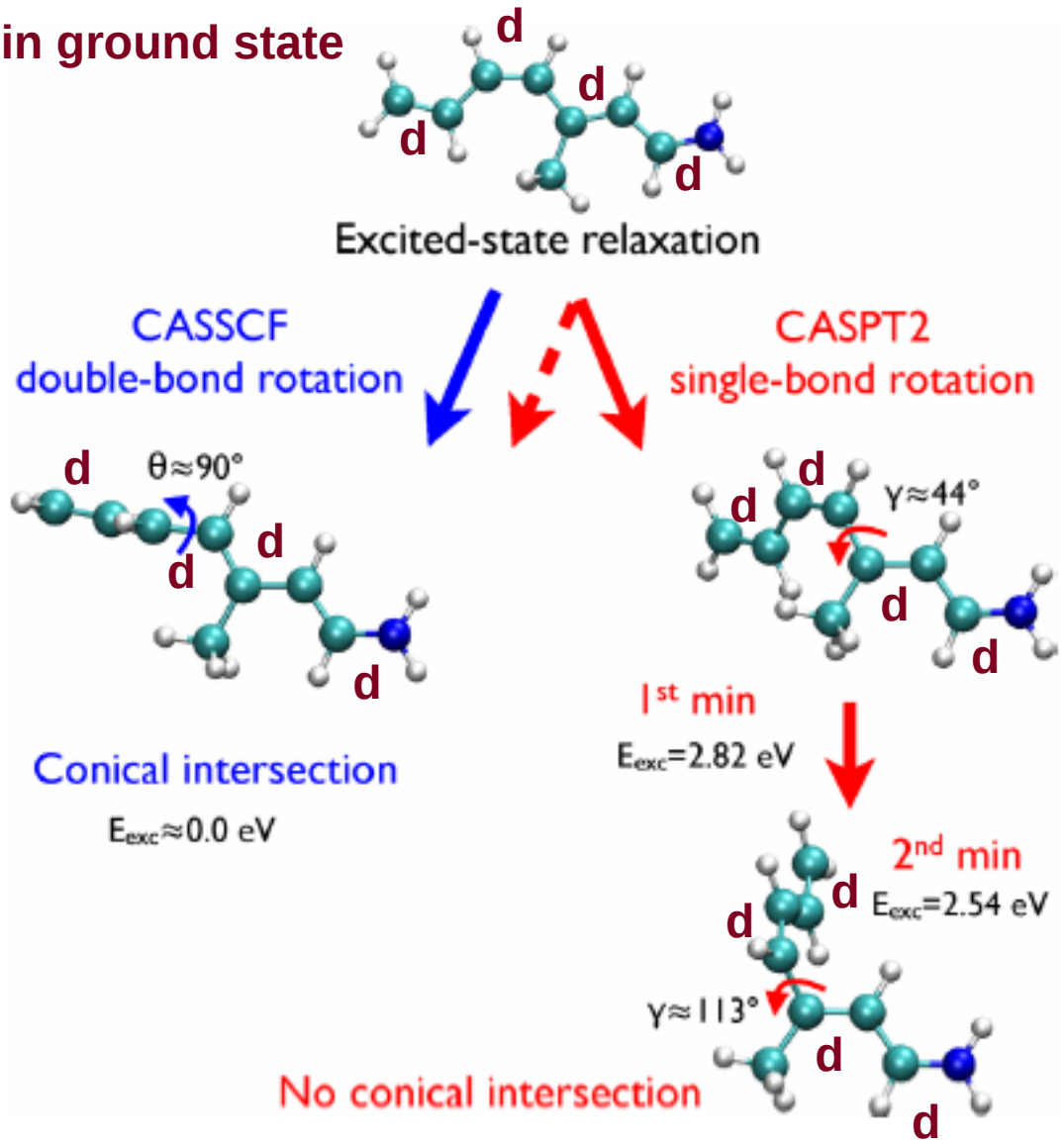

FIG. 1. The excited-state out-of-plane minima obtained with CASSCF and CASPT2. The solid arrows indicate MEPs while the dashed (red) arrow indicates the presence of a transition state on the S_1 surface.

CASPT2

$\theta = -10^o$

$\gamma = 43.6^o$

B3LYP	CAM-B3LYP
---	---

LC-BLYP

$\theta = -27.4^o$

$\gamma = 17.7^o$

CASPT2

$\theta = 8.1^o$

$\gamma = 112.7^o$

B3LYP	CAM-B3LYP
$\theta = -2.4^o$	$\theta = -1.2^o$
$\gamma = 85.4^o$	$\gamma = 85.2^o$

LC-BLYP

$\theta = -0.2^o$

$\gamma = 86.8^o$

Λ-Criterion*

$$\Lambda = \frac{\sum_{i,a} \kappa_{ia}^2 O_{ia}}{\sum_{i,a} \kappa_{ia}^2} \qquad (1)$$

$$\kappa_{ia} = X_{ia} + Y_{ia} \qquad (2)$$

$$O_{ia} = \int |\psi_i(\vec{r})||\psi_a(\vec{r})| d\vec{r} \qquad (3)$$

Small values (< 0.3) of Λ indicate a high likelihood of a "charge-transfer" underestimation.

* M.J.G. Peach, P. Benfield, T. Helgaker, and D.J. Tozer, *J. Chem. Phys.* **128**, 044118 (2008). "Excitation energies in density functional theory: An evaluation and a diagnostic test"

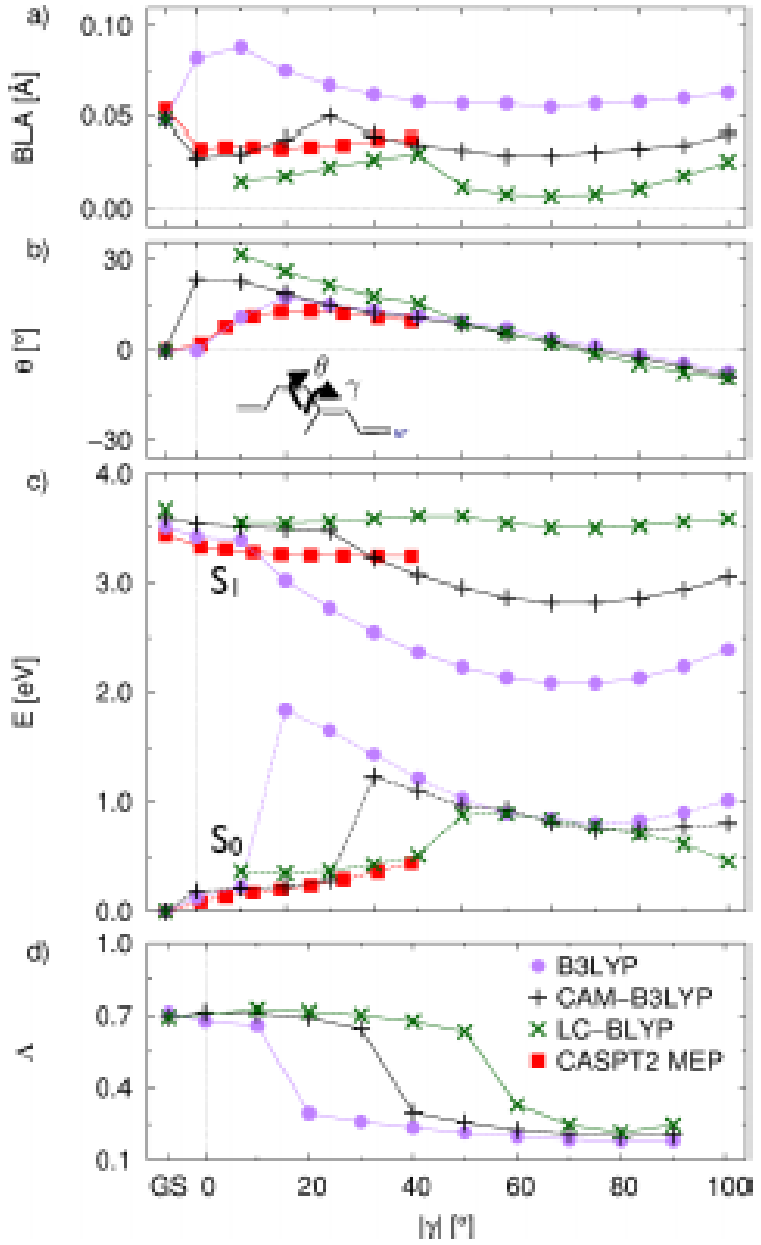

FIG. 6. Constrained geometrical excited-state optimization of the PSB4(1) model (C) for fixed torsional angle γ (formal single-bond rotation) obtained within TD-DFT. The CASPT2 MEP as a function of the torsional angle γ is also shown. We plot the BLA (panel (a)), the torsional angles θ for double-bond rotations (panel (b)), and the ground- and excited-state energies along the paths (panel (c)), and the Λ values along the TD-DFT paths (panel (d)).

Scan around single bond

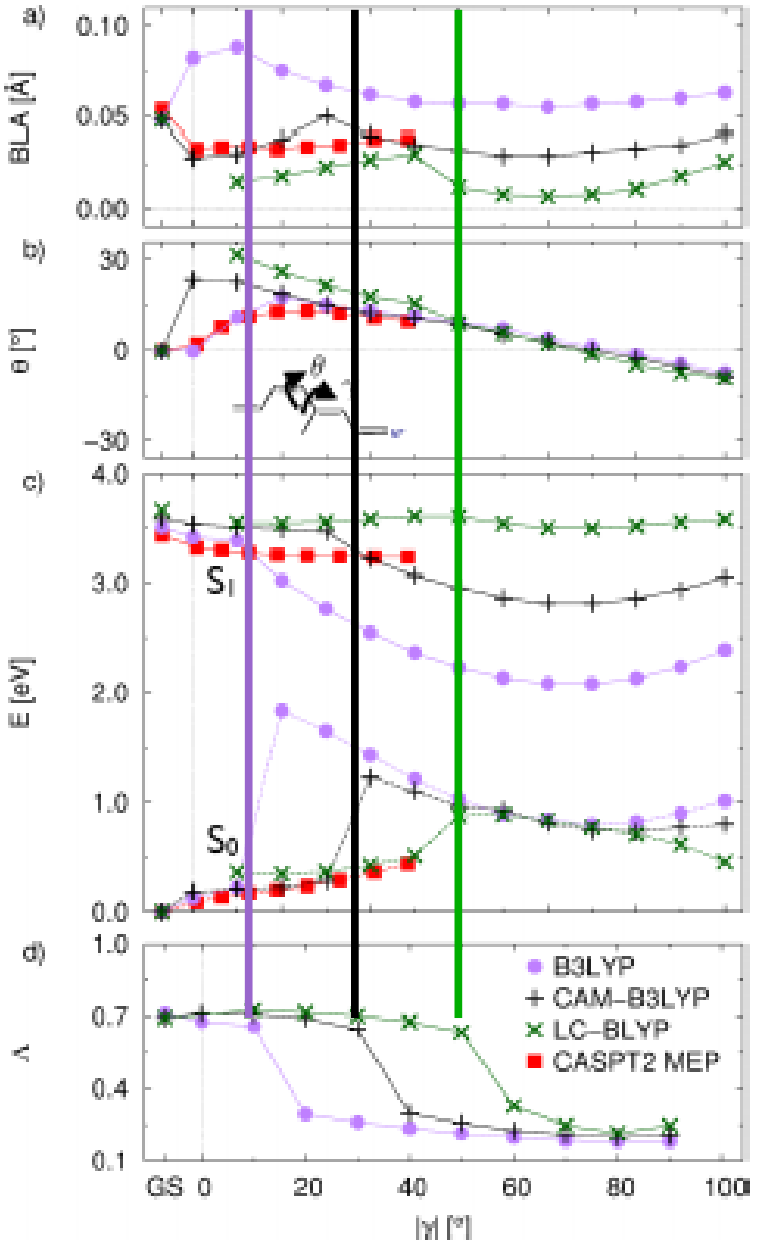

FIG. 6. Constrained geometrical excited-state optimization of the PSB4(1) model (C) for fixed torsional angle γ (formal single-bond rotation) obtained within TD-DFT. The CASPT2 MEP as a function of the torsional angle γ is also shown. We plot the BLA (panel (a)), the torsional angles θ for double-bond rotations (panel (b)), and the ground- and excited-state energies along the paths (panel (c)), and the Λ values along the TD-DFT paths (panel (d)).

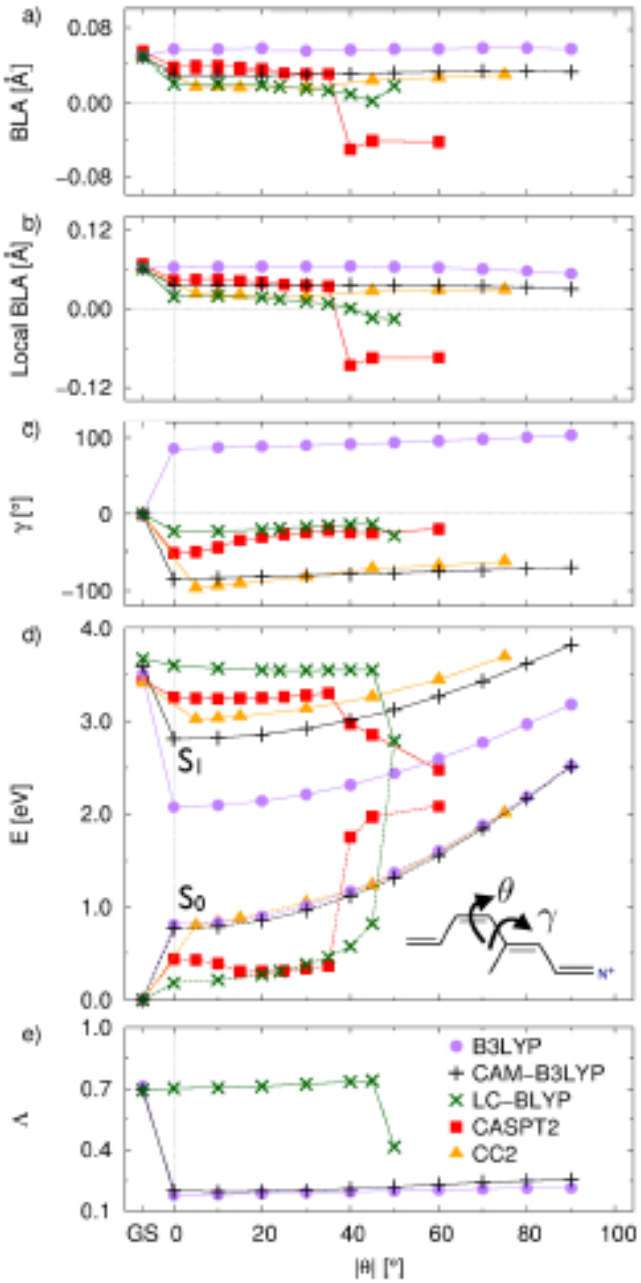

FIG. 5. Constrained geometrical excited-state optimization of the PSB4(1) model (C) for fixed torsional angle θ (formal double-bond rotation) obtained within TD-DFT and CASPT2. We plot the BLA (panel (a)), the local BLA which gives the bond inversion of the C_{11}–C_{12} bond with respect to the two adjacent single bonds (panel (b)), the torsional angles γ for single-bond rotations (panel (c)), the ground- and excited-state energies (panel (d)), and the Λ values along the TD-DFT paths (panel (e)).

Scan around double bond

So close to the conical Intersection!?

Adv. Electr. Struc. Theory, Paris 2015

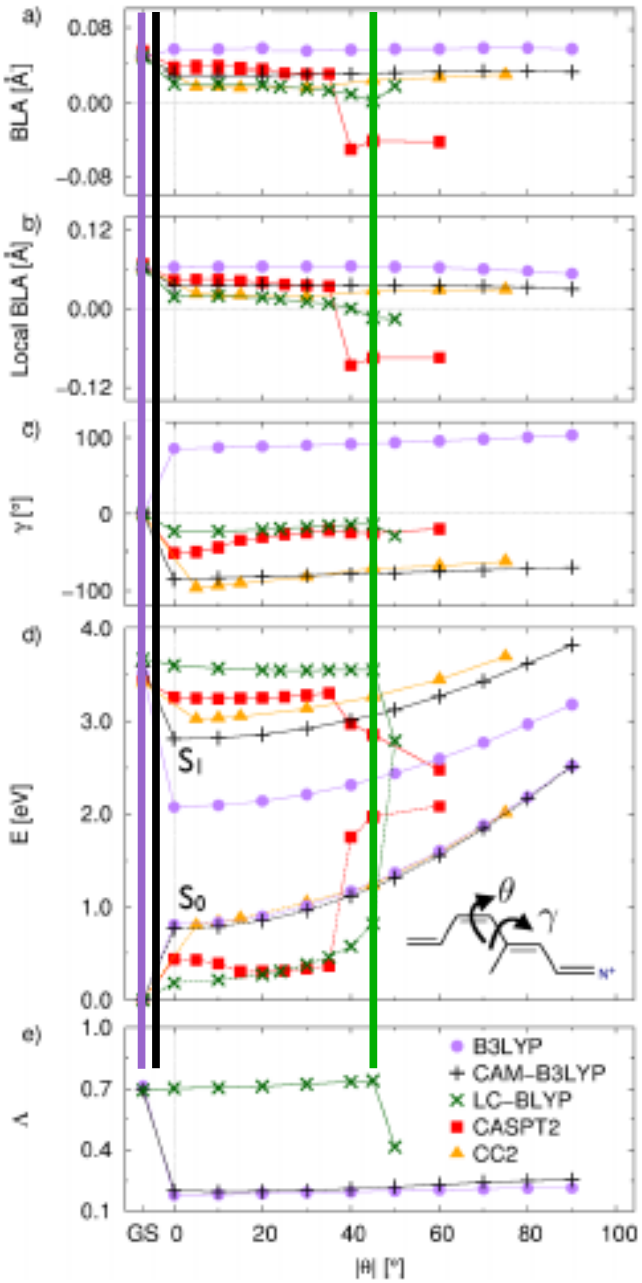

FIG. 5. Constrained geometrical excited-state optimization of the PSB4(1) model (C) for fixed torsional angle θ (formal double-bond rotation) obtained within TD-DFT and CASPT2. We plot the BLA (panel (a)), the local BLA which gives the bond inversion of the C_{11}–C_{12} bond with respect to the two adjacent single bonds (panel (b)), the torsional angles γ for single-bond rotations (panel (c)), the ground- and excited-state energies (panel (d)), and the Λ values along the TD-DFT paths (panel (e)).

RETINAL PSB CONCLUSION

- Earlier conclusions that (TD-)DFT failed for retinal PSB were largely based on insufficiently accurate *ab initio* calculations.
- (TD-)DFT, properly applied, works better than expected because charge-transfer errors are now "easy" to detect and correct.
- Also very important is that the double bond twist is not on the MEP.
- The expected failure for twisting around the double bond is indeed seen.

TABLE III. TD-DFT excitation energies of the first singlet (S_1) and triplet (T_1) excited states of the PSB4(1) model (C), computed with B3LYP, CAM-B3LYP, and LC-BLYP along the corresponding constrained excited-state geometries optimized for fixed torsional angle θ.

	B3LYP		CAM-BLYP		LC-BLYP	
θ (°)	S_1	T_1	S_1	T_1	S_1	T_1
GS	3.51	1.53	3.59	1.25	3.67	0.69
0	1.27	1.23	3.48	1.02	3.41	−0.48
10	1.26	1.23	2.03	1.82	3.35	−0.56
20	1.24	1.21	2.00	1.74	3.27	−0.72
30	1.20	1.16	1.96	1.59	3.16	−0.90
40	1.14	1.10	1.89	1.38	2.97	−1.10
50	1.07	1.03	1.81	1.07	0.00	−0.00
60	0.99	0.94	1.71	0.54	...	...
70	0.89	0.79	1.59	−0.74	...	...
80	0.78	−0.26	1.45	−1.13	...	...
90	0.66	−0.85	1.31	−1.34	...	...

I. Gaming Levels
II. (TD-)DFT
III. Retinal Schiff Base
IV. Dressed-TD-DFT
V. Conclusions

$$\begin{bmatrix} \omega_S & x \\ x & \omega_D \end{bmatrix} \begin{pmatrix} C_S \\ C_D \end{pmatrix} = \omega \begin{pmatrix} C_S \\ C_D \end{pmatrix} \qquad (1)$$

$$\omega = \omega_S + \frac{x^2}{\omega - \omega_D} \qquad (2)$$

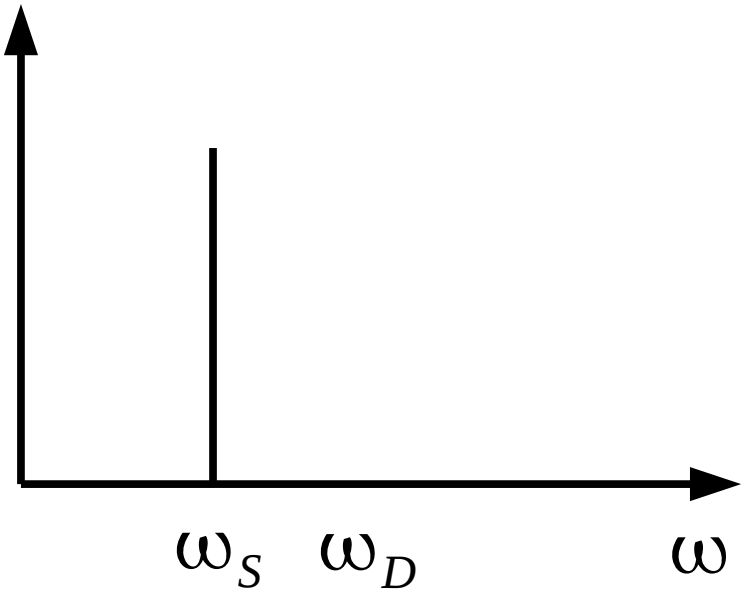

Static correlation

$$\Delta = \frac{x^2}{\omega_D - \omega_S}$$

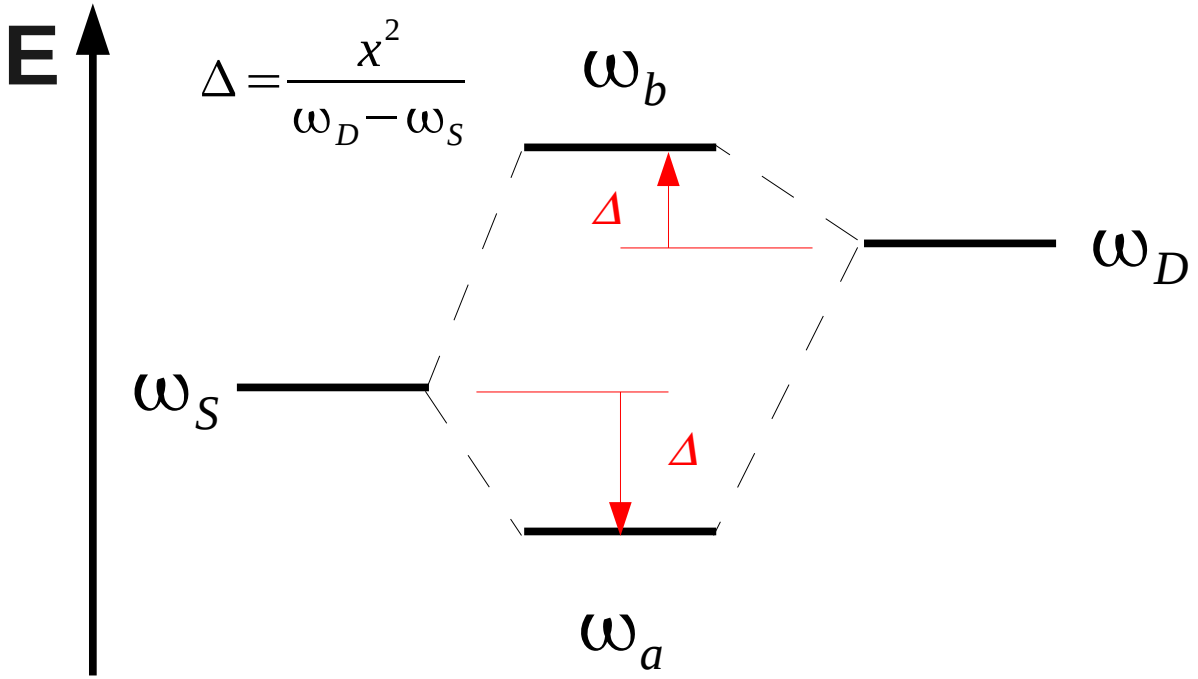

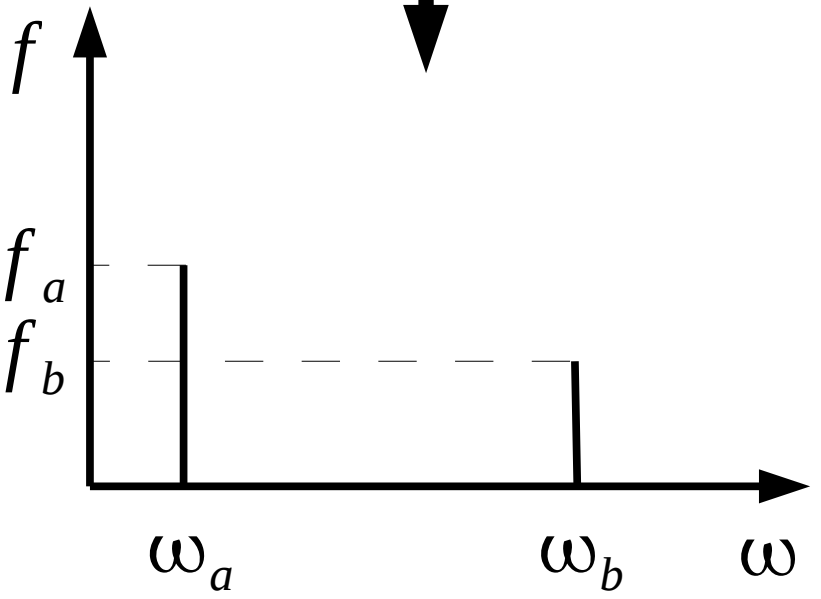

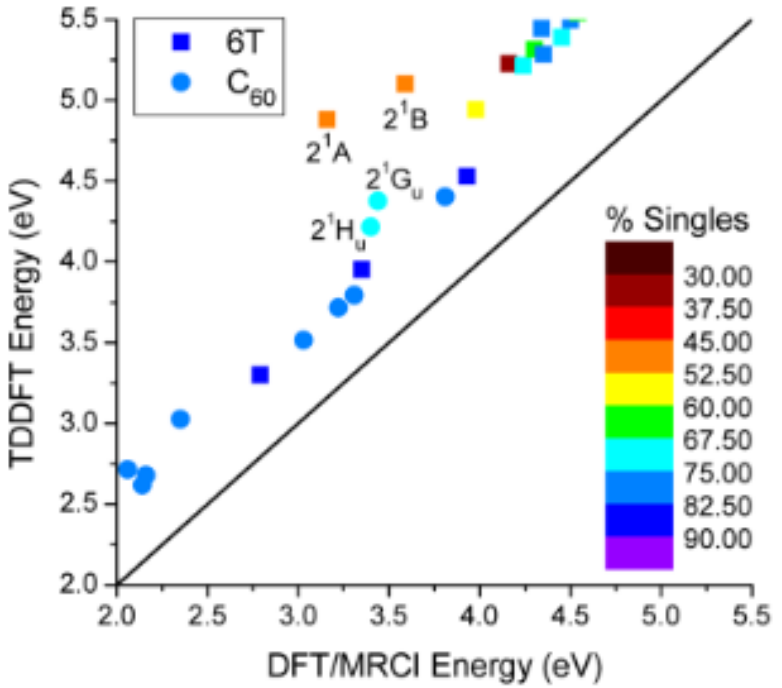

Figure 5. Excited-state energies of 6T and C_{60} computed with TD-ωB97X-D/6-31G(d) in comparison to the energies computed with the DFT/MRCI/SV(P) method. The color code indicates the total fraction of single excitations for each state.

K. Sen, R. Crespo-Otero, O. Weingart, W. Thiel, and M. Barbatti, *J. Chem. Theory Comput.* **9**, 533 (2013). **Interfacial states in donor-aceptor organic heterojunctions: Computational insights into thiophene-oligomer/fullerene junctions.**

THE ORIGINAL IDEA

N.T. Maitra, F. Zhang, R.J. Cave, and K. Burke, "Double excitations within time-dependent density-functional theory linear reponse theory", *J. Chem. Phys.* **120**, 5932 (2004).

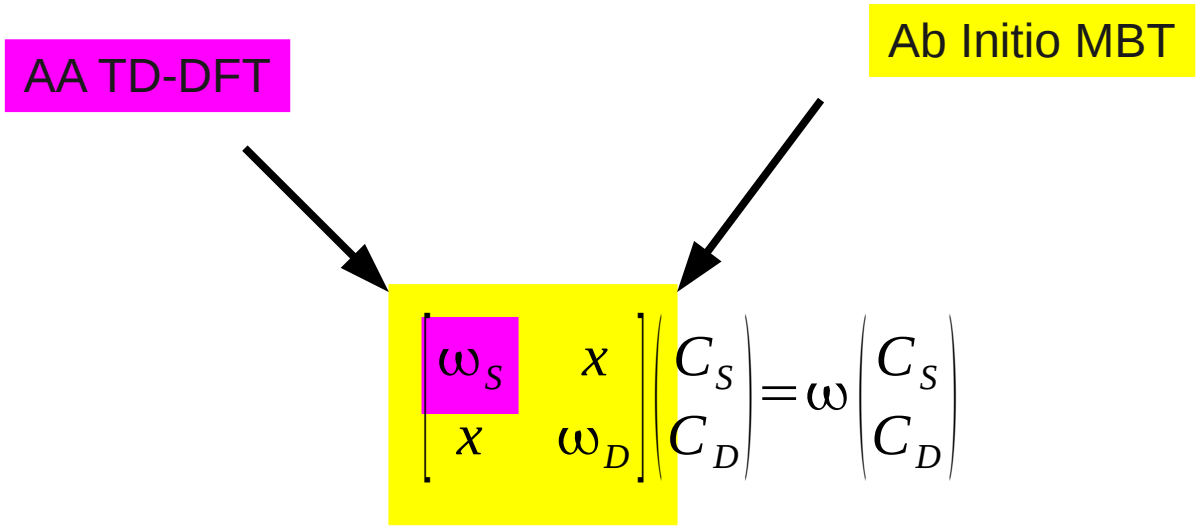

- What functional for AA TD-DFT?
- What level of MBT?
- How to implement?
- Extensive testing?

Miquel Huix-Rotllant: Improvement of TDDFT Modeling of the Spectroscopy of Nanosystems Through Better Understanding of the Space-Time Trade-Off in the Exchange-Correlation Functional

Miquel Huix-Rotllant, A. Ipatov, A. Rubio, and M.E. Casida, "Assessment of Dressed Time-Dependent Density-Functional Theory for the Low-Lying Valence States of 28 Organic Chromophores", *Chem. Phys.* **391**, 120 (2011).

M.E. Casida and Miquel Huix-Rotllant, *Topics in Current Chemistry*, special volume on Density-Functional Methods for Excited States, edited by N. Ferré, M. Filatov, and M. Huix-Rotllant, *in press*
Many-Body Perturbation Theory (MBPT) and Time-Dependent Density-Functional Theory (TD-DFT): MBPT Insights About What is Missing in, and Corrections to, the TD-DFT Adiabatic Approximation

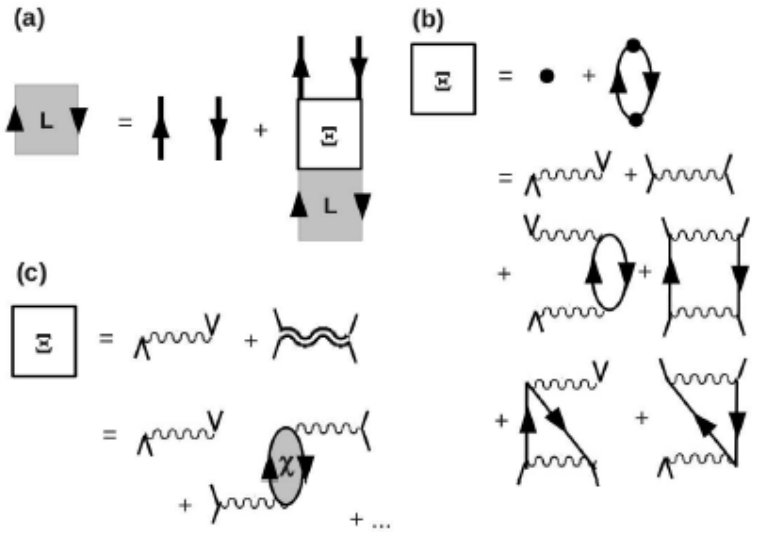

Fig. 10 Time-unordered (Feynman and Abrikosov) ph-propagator diagrams: (a) BSE, (b) secon order self-energy quantum chemistry approximation, (c) *GW* self-energy solid-state physics a proximation. Note in part (c) that the solid-state physics literature will often turn the *v* and wiggly lines at right angles to each other to indicate the same thing that we have indicated here adding tab lines.

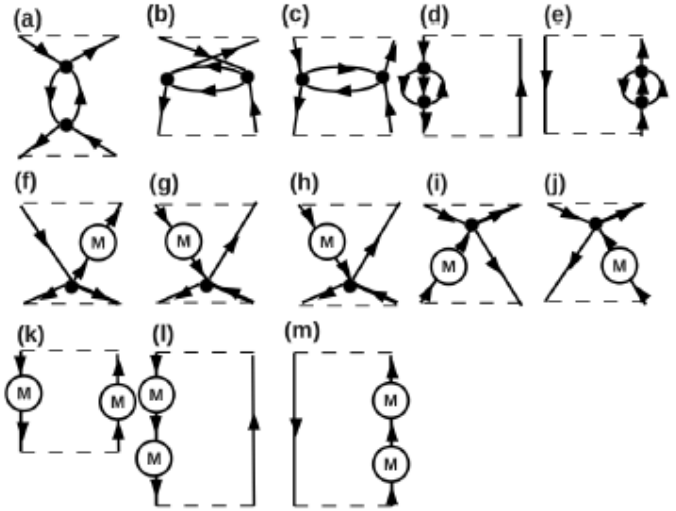

Fig. 12 Second-order time-unordered Abrikosov PP diagrams. Not all of the time-ordered Hugenholtz diagrams are generated by our procedure—only about 140 Hugenholtz diagrams.

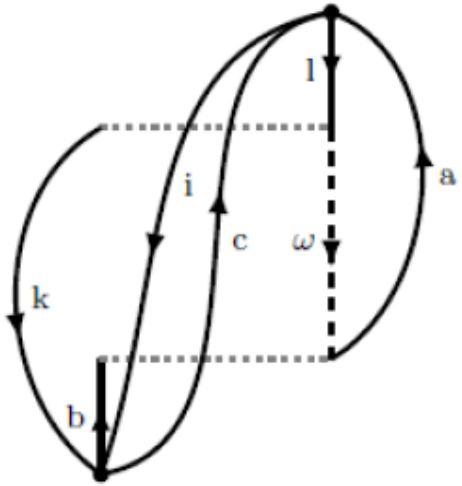

Fig. 13 An example of a second-order time-ordered Hugenholtz PP diagrams.

M.E. Casida and Miquel Huix-Rotllant, *Topics in Current Chemistry*, special volume on Density-Functional Methods for Excited States, edited by N. Ferré, M. Filatov, and M. Huix-Rotllant, *in press*

Many-Body Perturbation Theory (MBPT) and Time-Dependent Density-Functional Theory (TD-DFT): MBPT Insights About What is Missing in, and Corrections to, the TD-DFT Adiabatic Approximation

$$\left[\boldsymbol{A}_{1,1}^{(0+1+2)}\right]_{kc,ia} = -\delta_{i,k}\delta_{a,c}\epsilon_{i,a} + (kc|f_{Hxc}|ia) \qquad (1)$$

AA TDA TD-DFT

$$\left[\boldsymbol{A}_{2,1}^{(1)}\right]_{kc,jbia} = -\delta_{i,k}(bc||aj) + \delta_{j,k}(bc||ai) - \delta_{b,c}(ai||kj) + \delta_{k,j}(bi||kj) \qquad (2)$$

$$\left[\boldsymbol{A}_{2,2}^{(0)}\right]_{ldkc,jbia} = \delta_{j,l}\delta_{i,k}\delta_{c,a}\delta_{d,b}(\epsilon_a + \epsilon_b - \epsilon_i - \epsilon_j) \qquad (3)$$

D-TD-DFT => not good enough

Must violate order-consistency a bit! => x-D-TDDFT

$$\left[\boldsymbol{A}_{2,2}^{(1)}\right]_{aibj,ckdl} = \delta_{i,k}\delta_{j,l}\left(\delta_{a,c}F_{b,d}^{(0+1)} + \delta_{b,d}F_{a,c}^{(0+1)}\right) - \delta_{a,c}\delta_{b,d}\left(\delta_{j,l}F_{i,k}^{(0+1)} - \delta_{i,k}F_{d,l}^{(0+1)}\right) \qquad (4a.1)$$

$$-\delta_{a,c}f(b,d) - \delta_{b,d}f(a,c) + \delta_{a,d}f(b,c) + \delta_{b,c}f(a,d) \qquad (4a.2)$$

$$-\delta_{a,c}\delta_{b,d}(kj||li) - \delta_{j,l}\delta_{k,i}(ad||bc) \qquad (4a.3)$$

$$f(p,q) = \delta_{i,k}(lj||pq) + \delta_{j,l}(ki||pq) - \delta_{k,j}(li||pq) - \delta_{i,l}(kj||pq) \qquad (5)$$

“FORTRAN index convention”: $\underbrace{a,b,\cdots,h}_{virtual}\,\underbrace{i,j,\cdots,n}_{occupied}\,\underbrace{o,p,q,\cdots,z}_{free}$

M. Schreiber, M.R. Silva-Junior, S.P.A. Sauer, and W. Thiel, *J. Chem. Phys.* 128, 134110 (2008).
"Benchmarks for electronically excited states: CASPT2, CC2, CCSD, and CC3"

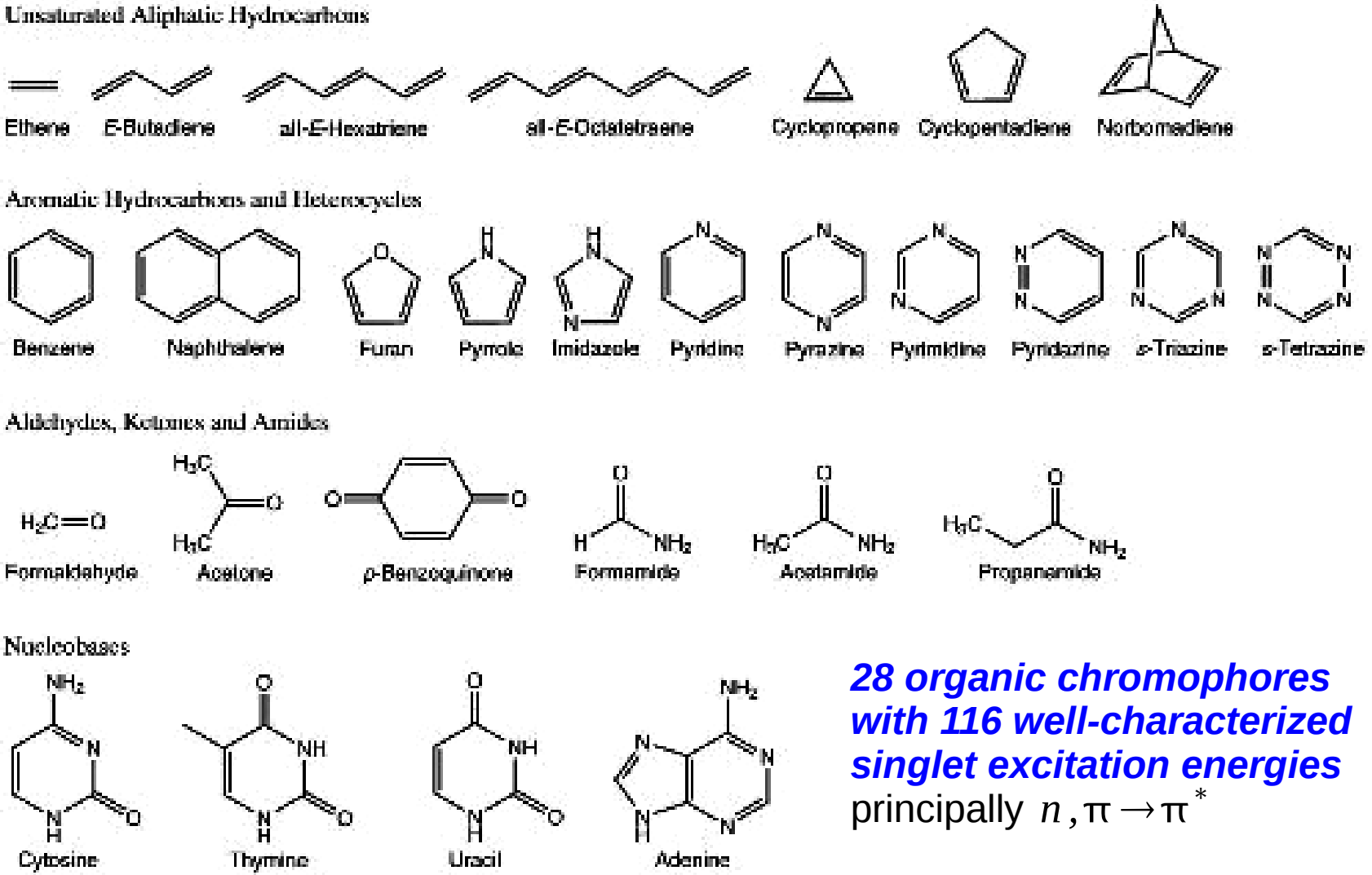

28 organic chromophores with 116 well-characterized singlet excitation energies
principally $n, \pi \rightarrow \pi^*$

EFFECT OF ADDING 10 DOUBLES

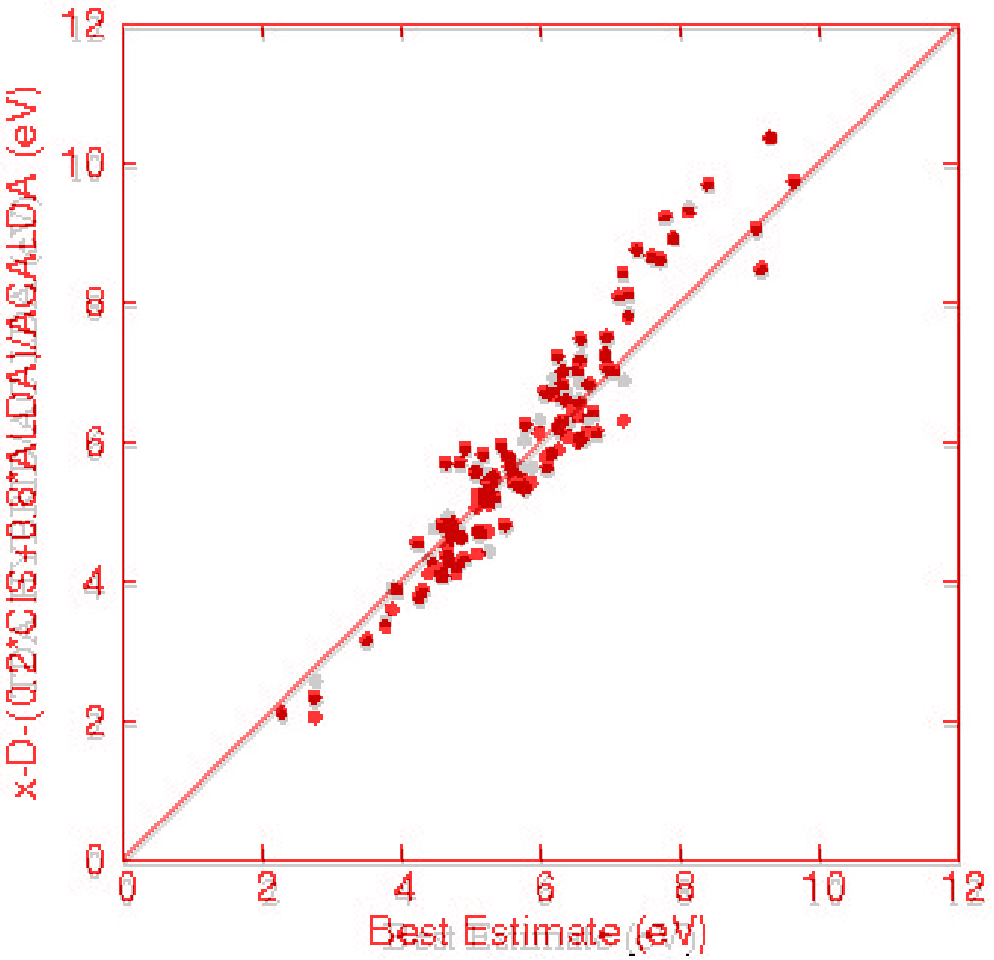

TDhybrid ≈ x-D-TDhybrid

TDhybrid ≈ x-D-TDhybrid

There is almost no difference! (This is a good thing.)

BUTADIENE CH_2=CH-CH=CH_2

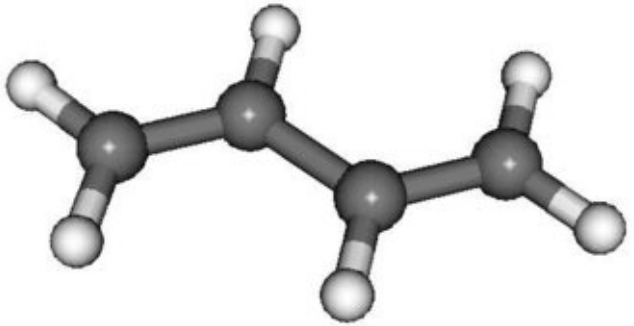

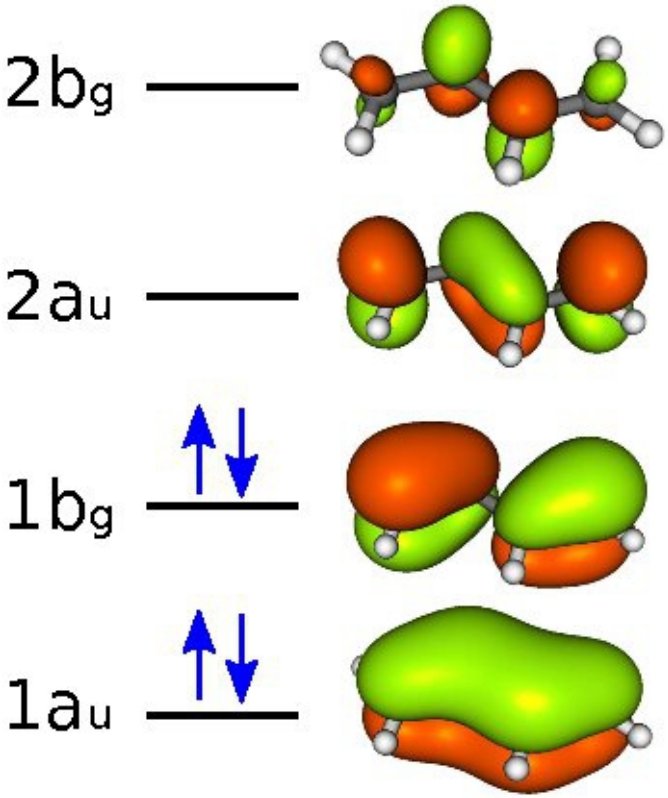

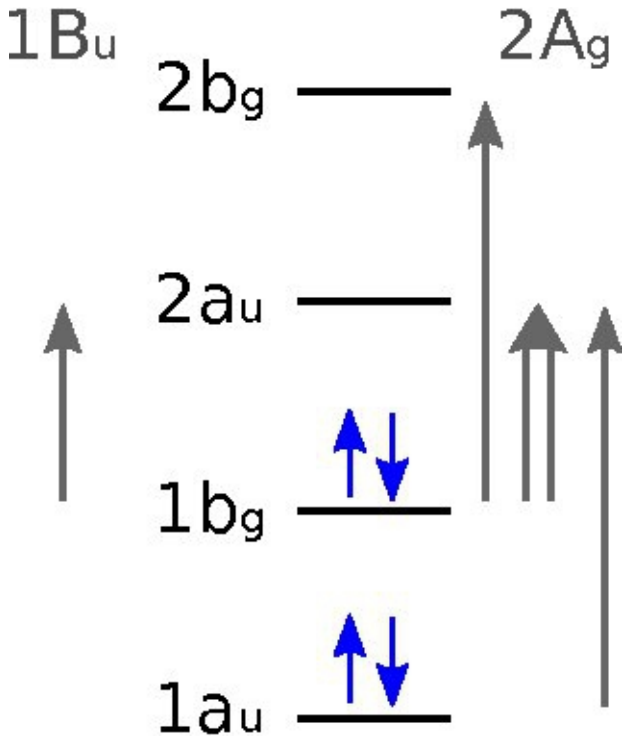

States having more than 10% doubles character according to CCSD calculations.

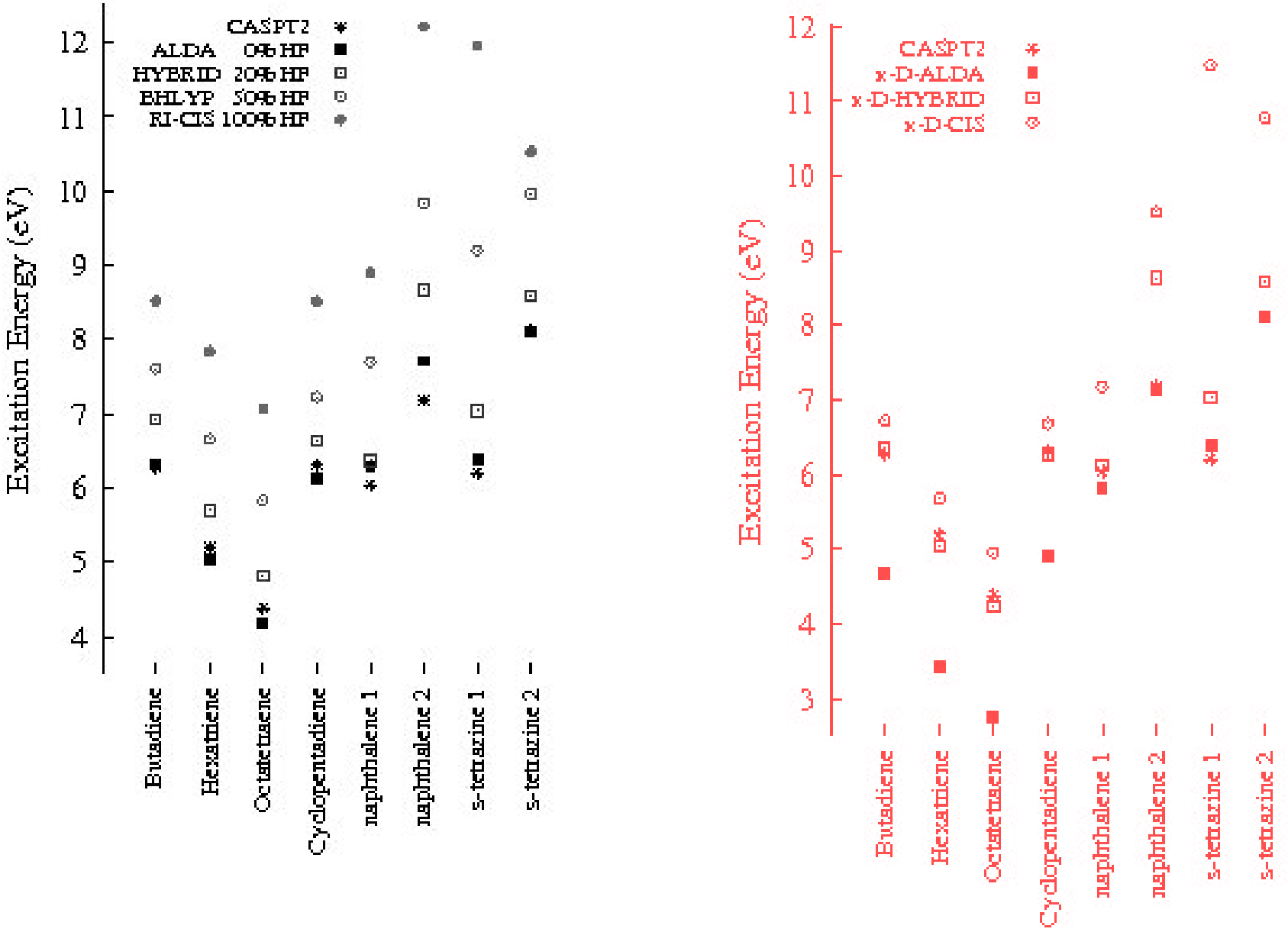

Miquel Huix-Rotllant, A. Ipatov, A. Rubio, and M.E. Casida, "Assessment of Dressed Time-Dependent Density-Functional Theory for the Low-Lying Valence States of 28 Organic Chromophores", *Chem. Phys.* **391**, 120 (2011).

IMPORTANT CONCLUSION: dressed-TD-DFT requires hybrid functionals

D-TDA-TD-DFT

singles →
doubles →

$$\begin{bmatrix} A_{1,1} & A_{1,2} \\ A_{2,1} & A_{2,2} \end{bmatrix} \begin{pmatrix} \vec{C}_1 \\ \vec{C}_2 \end{pmatrix} = \omega \begin{pmatrix} \vec{C}_1 \\ \vec{C}_2 \end{pmatrix} \qquad (1)$$

b-D-TDA-TD-DFT

GKS determinant →
singles →
doubles →

$$\begin{bmatrix} 0 & A_{0,1} & A_{0,2} \\ A_{1,0} & A_{1,1} & A_{1,2} \\ A_{2,0} & A_{2,1} & A_{2,2} \end{bmatrix} \begin{pmatrix} C_0 \\ \vec{C}_1 \\ \vec{C}_2 \end{pmatrix} = \omega \begin{pmatrix} C_0 \\ \vec{C}_1 \\ \vec{C}_2 \end{pmatrix} \qquad (2)$$

$$\left[A_{0,1}\right] = \langle j|\hat{M}_{xc}|b\rangle \neq 0 \qquad (3a)$$

$$\left[A_{0,2}\right] = 2\left[(kc|f_H|ld) - (kd|f_H|lc)\right] \qquad (3b)$$

H_2 SINGLET DISSOCIATION CURVES: Full CI/cc-pVTZ

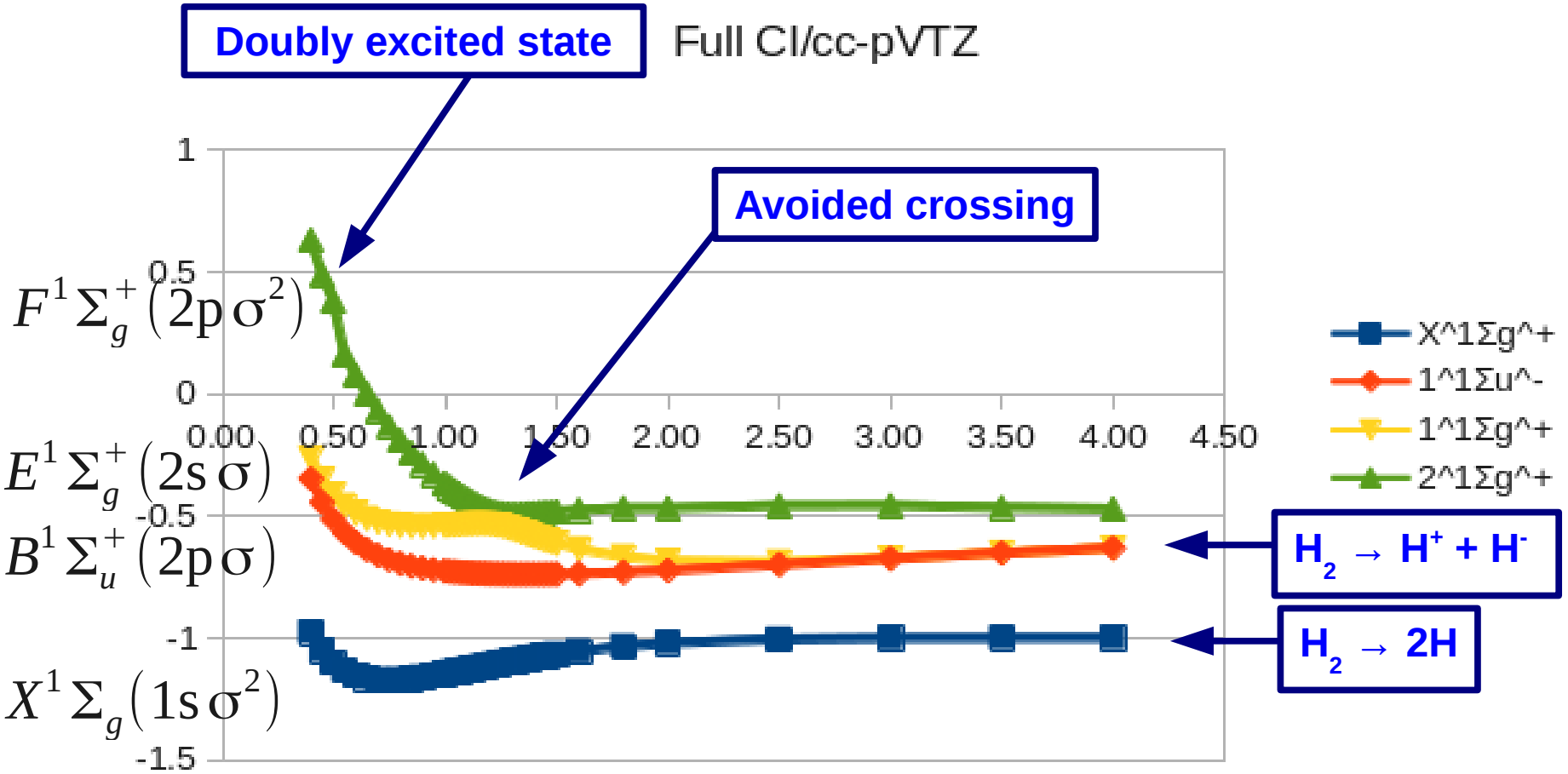

Not shown: $C^1\Pi_u(2p\pi)$

H_2 SINGLET DISSOCIATION CURVES: BHHLYP/cc-pVTZ

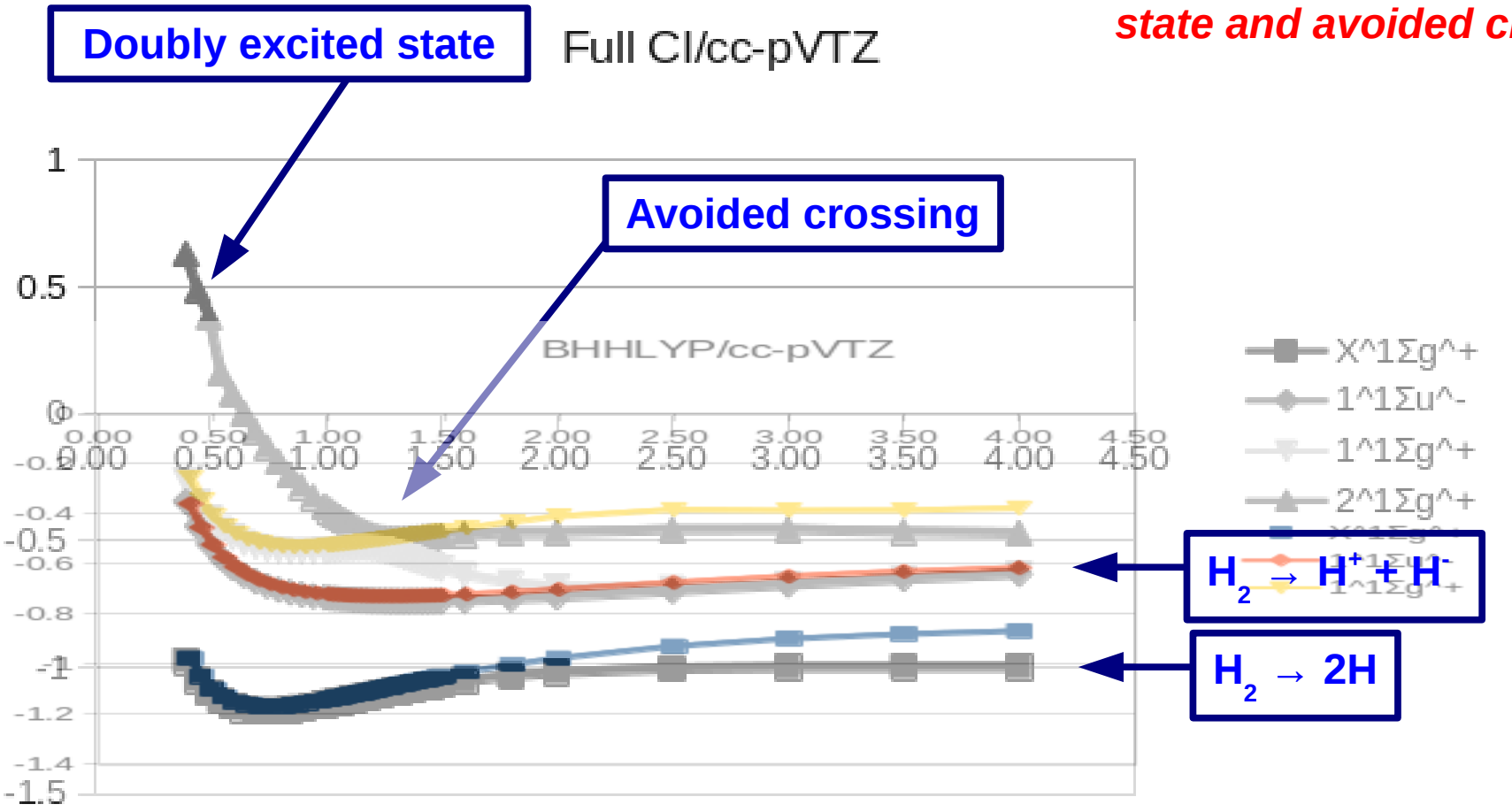

Missing doubly-excited state and avoided crossing

Incorrect ground-state dissociation

H_2 SINGLET DISSOCIATION CURVES : Dressed BHHLYP/cc-pVTZ + 1 HF-DEX

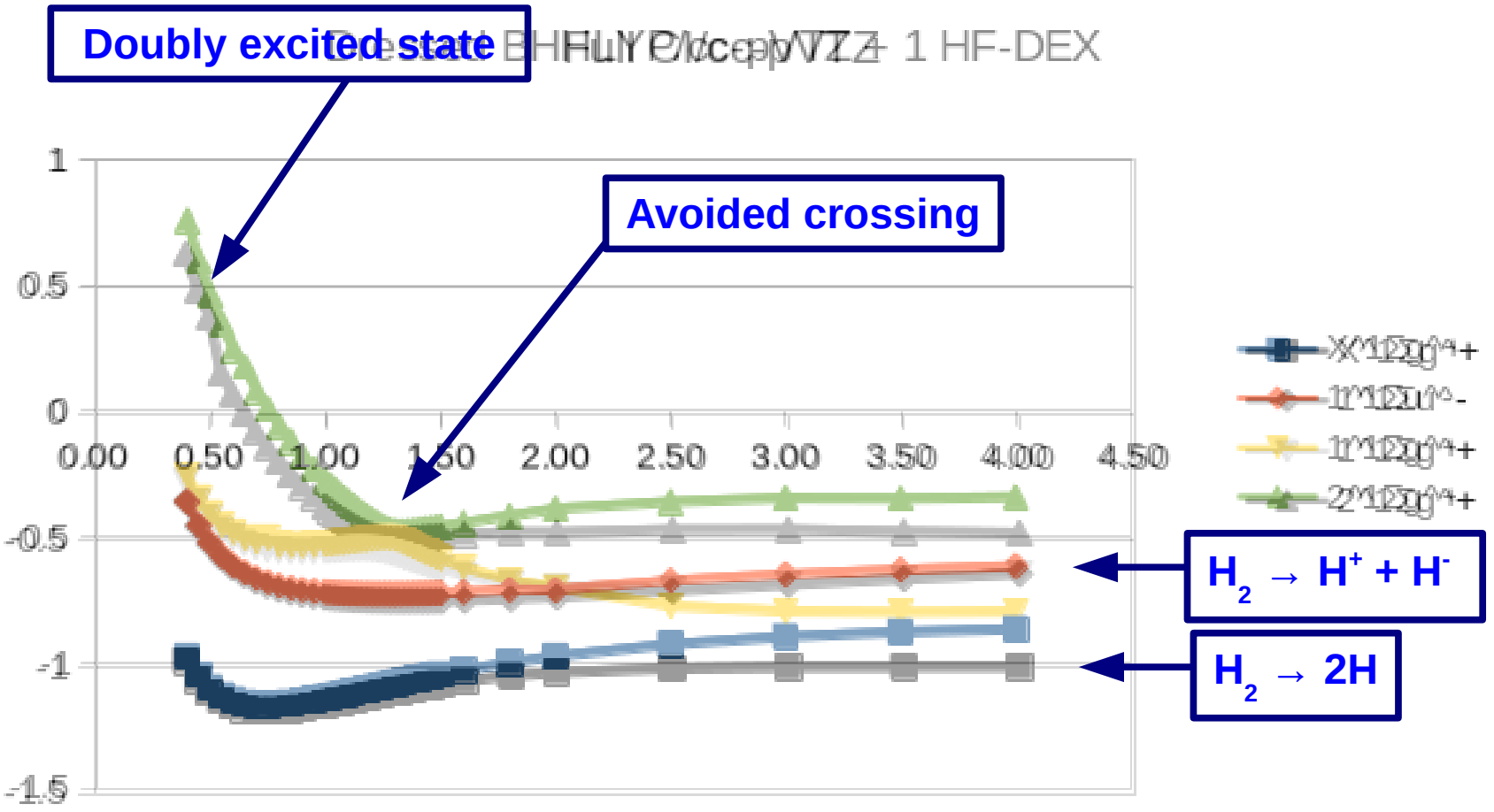

Incorrect ground-state dissociation

H_2 SINGLET DISSOCIATION CURVES : Dressed BHHLYP/cc-pVTZ + 1 HF-DEX + GS

$F^1\Sigma_g^+\left(2p\sigma^2\right)$

still has a "small" problem dissociating

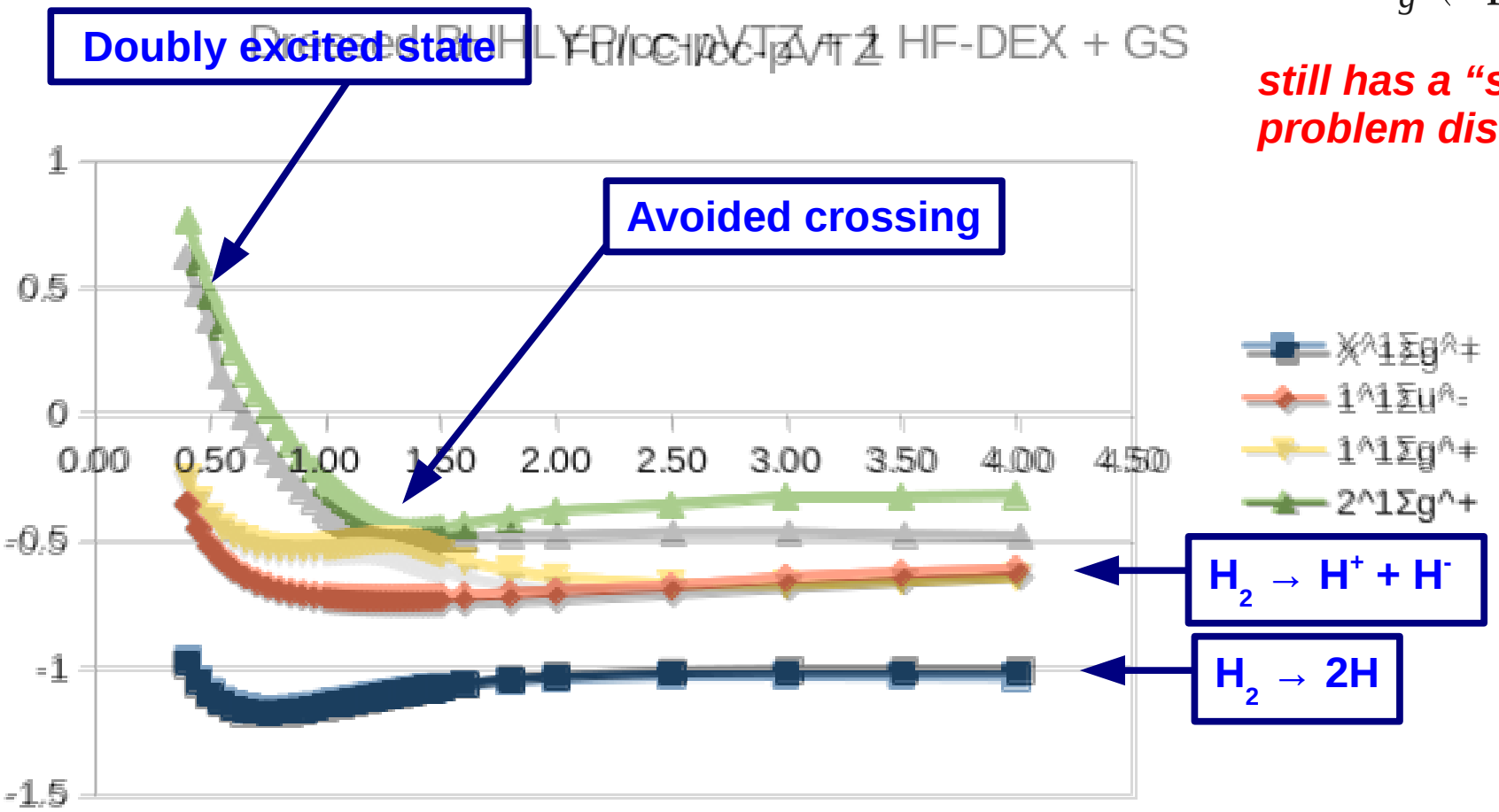

Fig. 1 Typical curves for the singlet photochemical isomerization of ethylene.

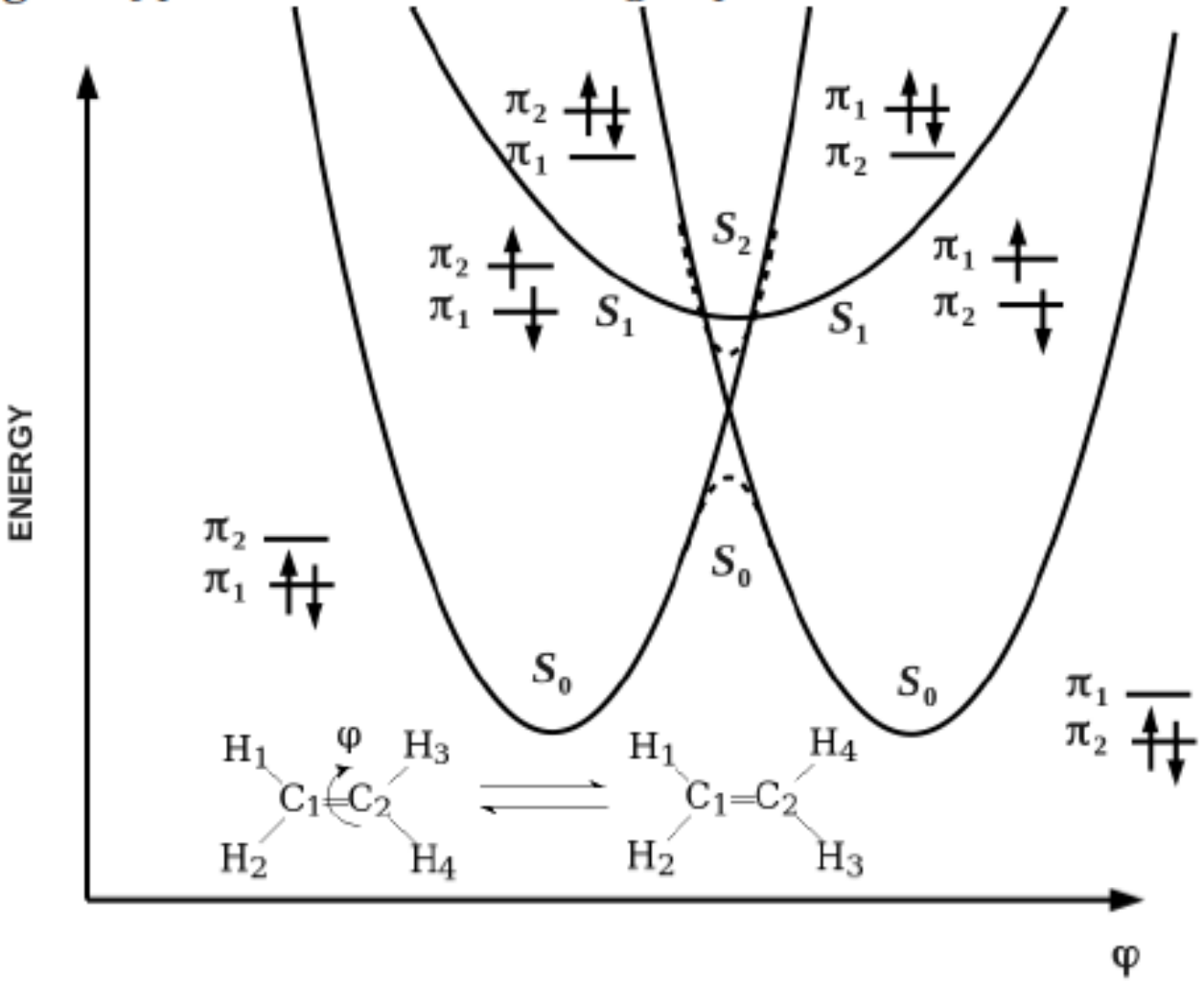

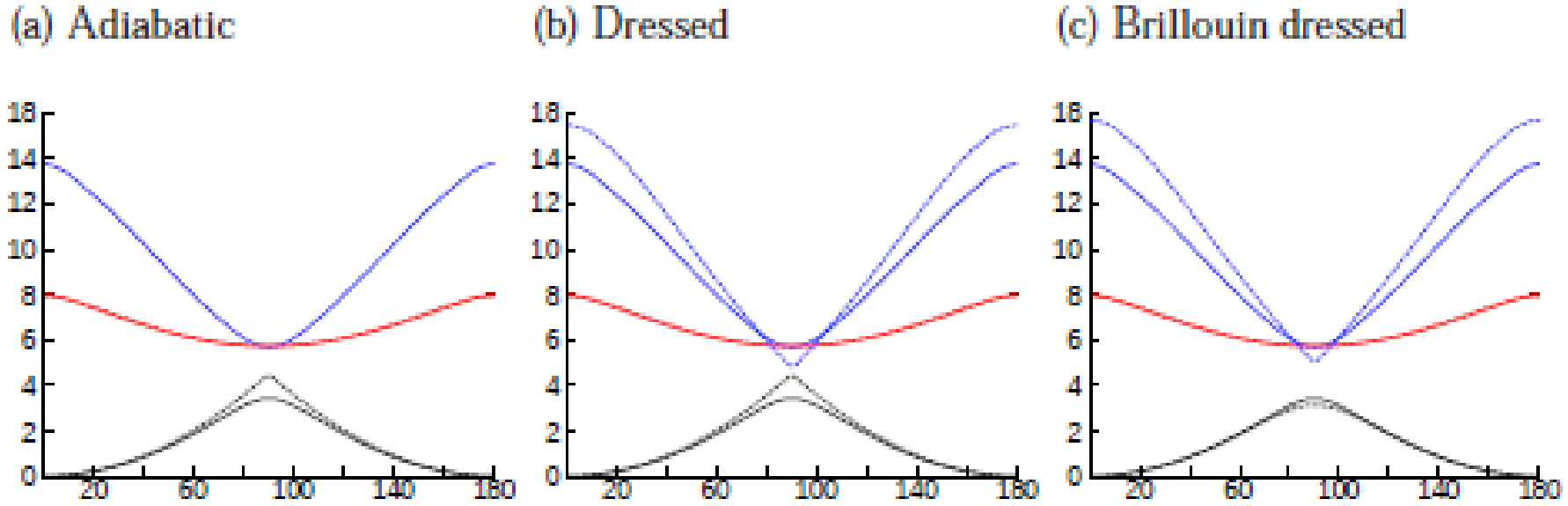

Fig. 17 Potential energy cuts of the S_0, S_1 and S_2 states of ethylene along the twisting coordinate: *x*-axis in degrees, *y*-axis in eV. All the curves have been shifted so that the ground-state curve at 0° corresponds to 0 eV. The solid lines correspond to a CASSCF(2,2)/MCQDPT2 calculation, and the dashed lines to the different models using the BH&HLYP functional and the Tamm-Dancoff approximation. The 6-31++G(d,p) basis set have been employed in all calculations. (Note that these curves are in good agreement with similar calculations previously reported in Fig. 7.3 of Chapter 7 of Ref. [69], albeit with a different functional.)

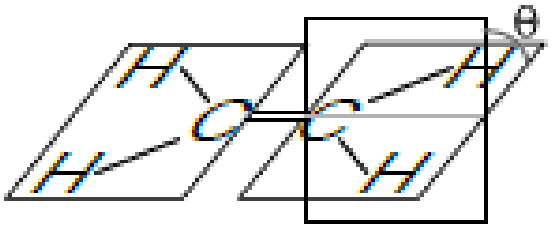

RELATED WORK …

S.L. Li, A.V. Marenich, X. Xu, and D.G. Truhlar, *J. Chem. Phys. Lett.* **5**, 322 (2014).
"Configuration interaction-corrected Tamm-Dancoff approximation: A time-dependent Density functional method with the correct dimensionality of conical intersections"

Same spirit as the Brillouin corrections in Miquel's 2011 thesis ...

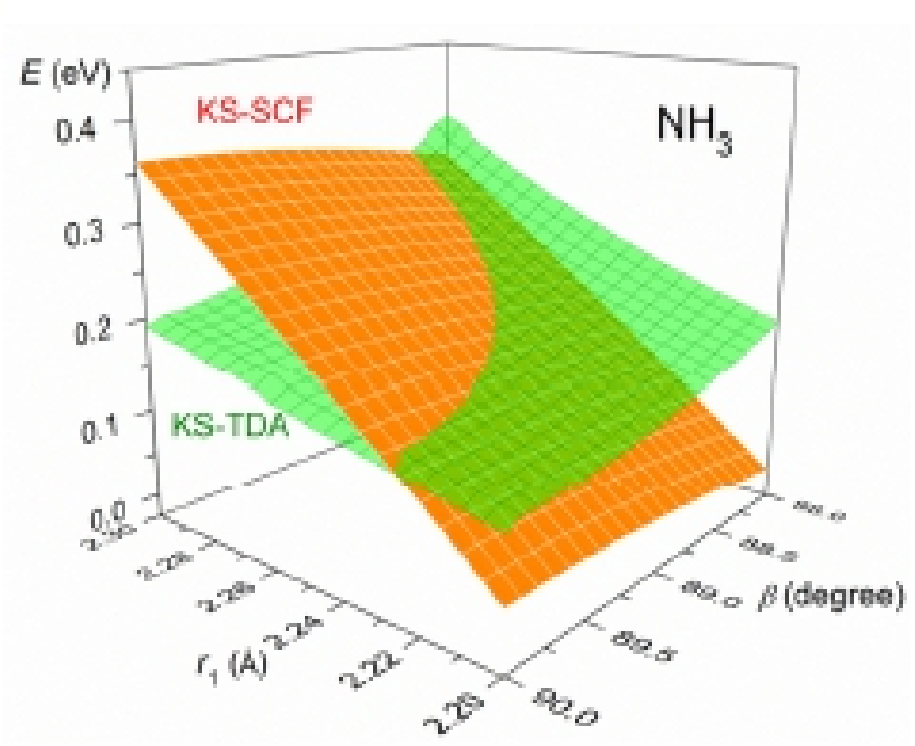

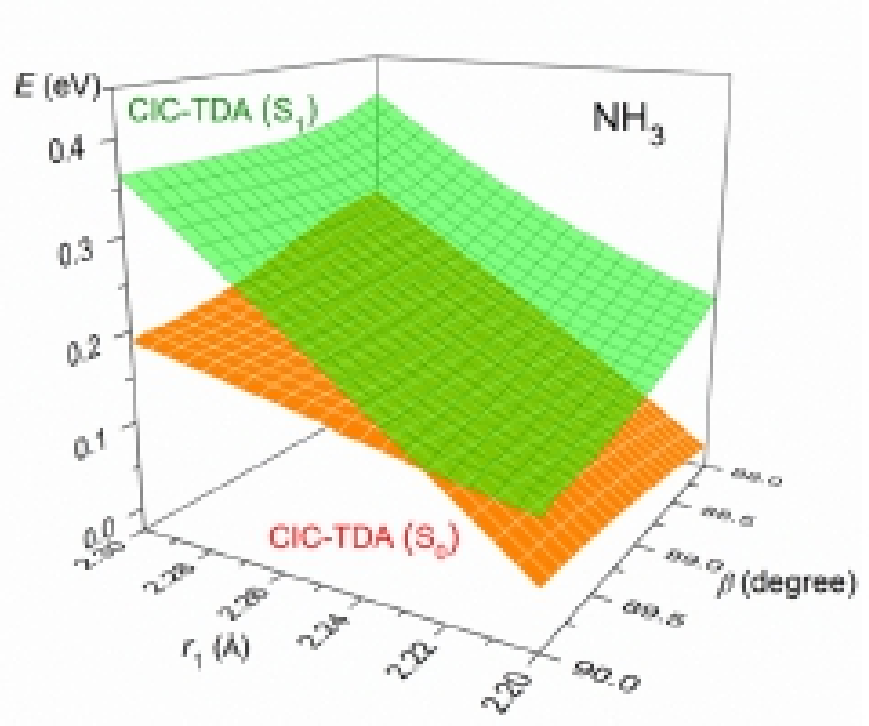

E. Fromager, S. Knecht, and H.J.Aa. Jensen, "Multi-configuration time-dependent density-functional theory based upon range separation," *J. Chem. Phys.* **138**, 084101 (2013).

$$\frac{1}{r_{12}} = \underbrace{\frac{erfc(\gamma r_{12})}{r_{12}}}_{SHORT\ RANGE} + \underbrace{\frac{erf(\gamma r_{12})}{r_{12}}}_{LONG\ RANGE}$$

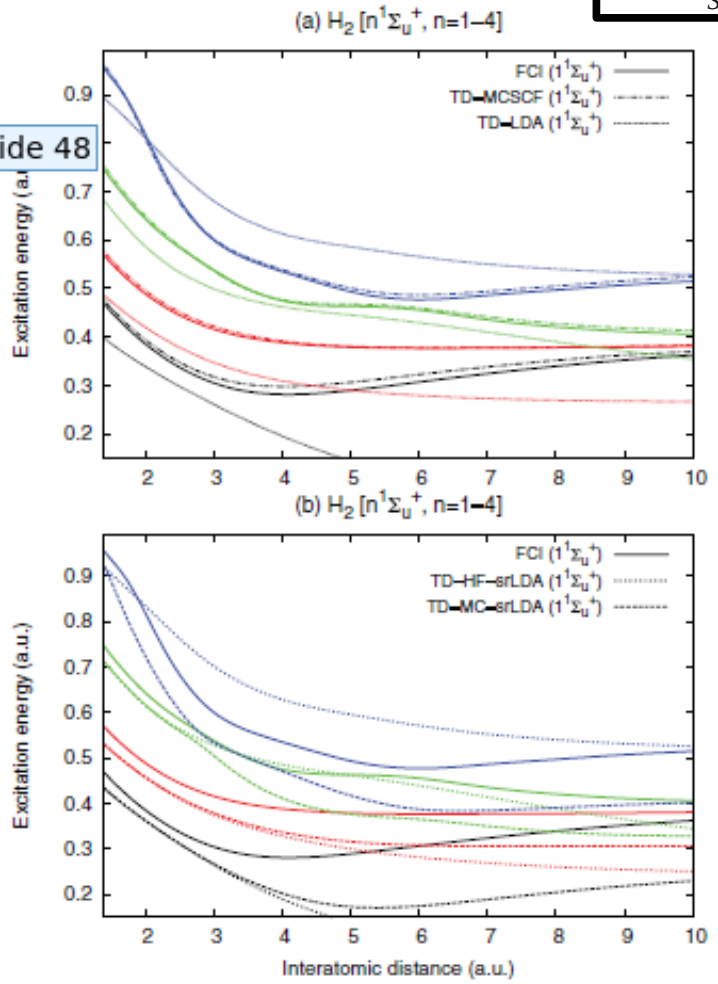

FIG. 1. First (black), second (red), third (green), and fourth (blue) $^1\Sigma_u^+$ excitation energies in H_2 along the bond-breaking coordinate calculated with minimal and TD-MCSCF and TD-LDA methods (b) TD-HF-srLDA and TD-MC-srLDA schemes. Comparison is made with FCI results. Each type of line corresponds to a given method. The μ parameter was set to 0.4 a.u. The minimal active space $1\sigma_g 1\sigma_u$ was used. Basis set is aug-cc-pVQZ.

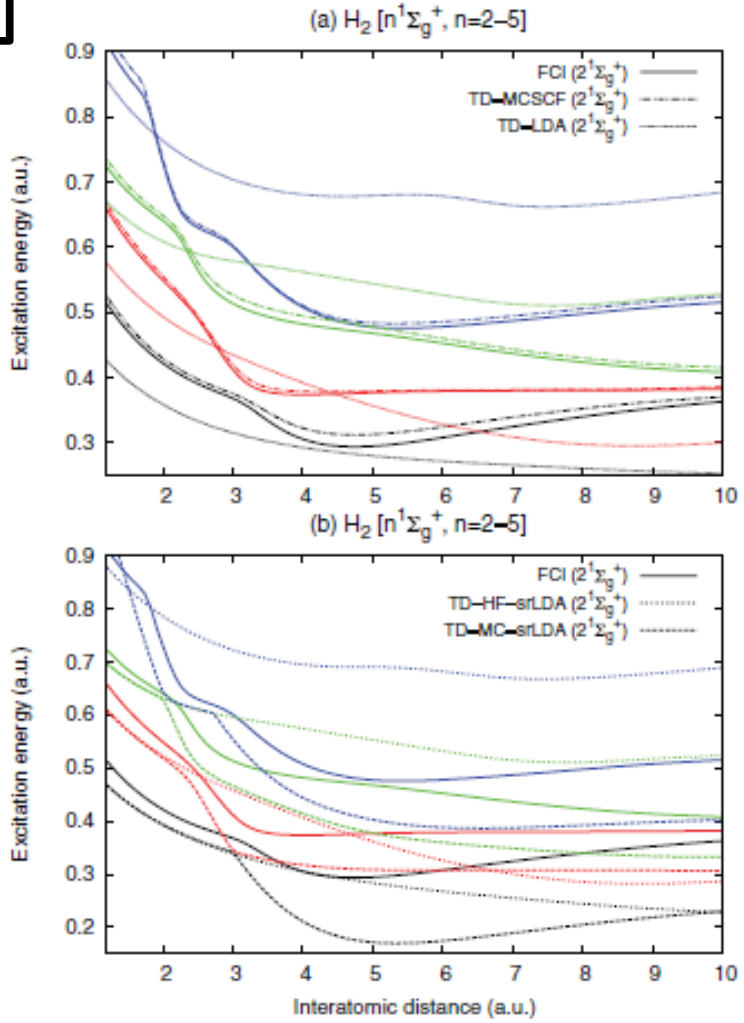

FIG. 2. First (black), second (red), third (green), and fourth (blue) $^1\Sigma_g^+$ excitation energies in H_2 along the bond-breaking coordinate calculated with (a) standard TD-MCSCF and TD-LDA methods (b) TD-HF-srLDA and TD-MC-srLDA schemes. Comparison is made with FCI results. Each type of line corresponds to a given method. The μ parameter was set to 0.4 a.u. The minimal active space $1\sigma_g 1\sigma_u$ was used. Basis set is aug-cc-pVQZ.

CONSTRICTED VARIATIONAL DFT

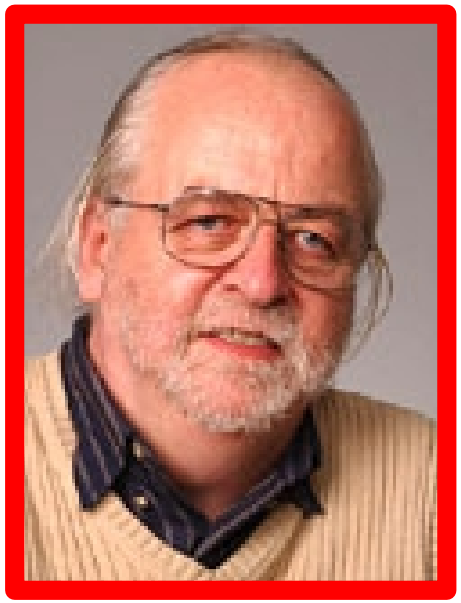

Tom Ziegler
1945-2015
RIP

T. Ziegler, M. Krykunov, and J. Autschbach, *J. Chem. Theory Comput.* **10**, 3980 (2014). "Derivation of the RPA equation of ATDDFT from and excited state variational approach based on the ground state functional"

M. Krykunov, M. Seth, and T. Ziegler, *J. Chem. Phys.* **140**, 18A502 (2014).

I. Seidu, M. Krykunov, and T. Ziegler, *Mol. Phys*. **112**, 661 (2014). "The formulation of a constricted variational density functional theory for double excitations"

M. Krykunov and T. Ziegler, *J. Chem. Theory Comput*. **9**, 2761 (2013).

M. Krykunov, S. Grimme, and T. Ziegler, *J. Chem. Theory Comput.* **8**, 4434 (2012).

T. Ziegler, M. Krykunov, and J. Cullen, *J. Chem. Phys*. **136**, 124107 (2012). "The implementation of a self-consistent constricted variational density functional theory for the description of excited states"

Exact theory

Ground state singlet belonging to the totally symmetric irrep

$\Rightarrow \quad \rho_\alpha = \rho_\beta \quad \Rightarrow \quad v_{xc}^{\alpha} = v_{xc}^{\beta} \quad \Rightarrow$ No symmetry breaking expected!

Assumes noninteracting v-representability (NVR)

NVR: There is a fictitious Kohn-Sham system of noninteracting electrons *with integer occupation number* whose ground state gives the density of the interacting system.

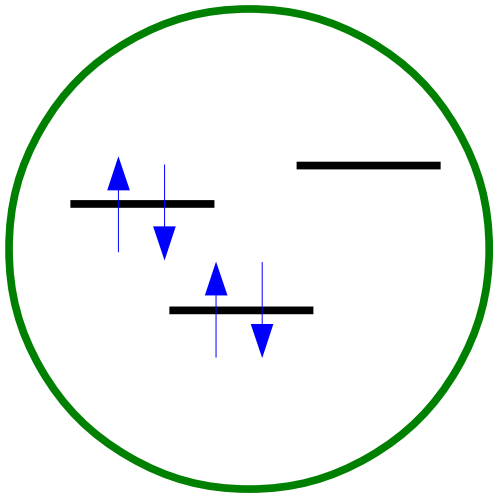

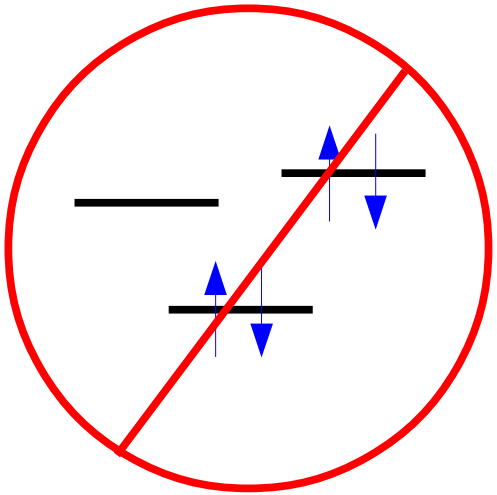

Traditional workaround is the ensemble formulation with fractional occupation numbers.

But this may lead to orbital-dependent potentials --- i.e., breakdown of the Kohn-Sham picture.

I. Gaming Levels
II. (TD-)DFT
III. Retinol Schiff Base
IV. Dressed-TD-DFT
V. Conclusions

CONCLUSION

(TD-)DFT is advancing faster than many users can keep up!

- The first events in photobiological systems appear to be within reach.
- Techniques are now being formulated which promise to take us even further.

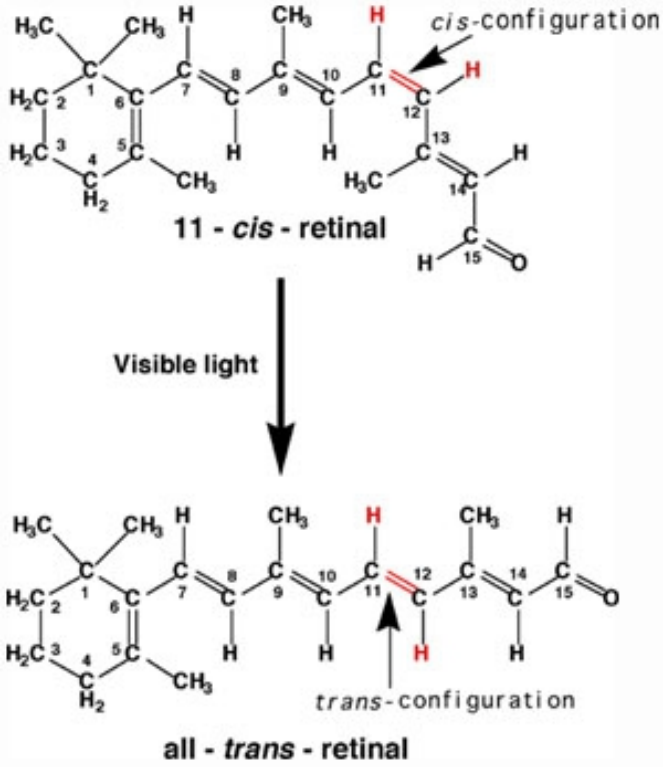

ACKNOWLEDGEMENTS

retinal PSB
We acknowledge the support from the *Stichting Nationale Computerfaciliteiten* (NCF-NWO) for the use of the SARA supercomputer facilities.

dressed-TD-DFT
We thank Andrei Ipatov, Valerio Olevano, Giovanni Onida, Lucia Reining, Pina Romaniello, Angel Rubio, Davide Sangalli, Jochen Schirmer, Eric Shirley, and Hemanadhan Myneni for useful discussions. M. H. R. would like to acknowledge an *Allocation de Recherche* from the French Ministry of Education. Over the years, this work has been carried out in the context of several programs: the French Rhône-Alpes *Réseau thématique de recherche Avancée* (*RTRA*): *Nanosciences aux limites de la nanoélectronique*, the Rhône-Alpes Associated Node of the European Theoretical Spectroscopy Facility (ETSF), and most recently the grant ANR-12-MONU-0014-02 from the French *Agence Nationale de la Recherche* for the ORGAVOLT project (ORGAnic solar cell VOLTage by numerical computation).